Title

MafF is an antiviral host factor that suppresses transcription from Hepatitis B Virus core promoter

Running title

MafF restricts viral replication

Authors

Marwa K. Ibrahim[1,2], Tawfeek H. Abdelhafez[1,2], Junko S. Takeuchi[1,3,4], Kosho Wakae[1], Masaya Sugiyama[5], Masataka Tsuge[6], Masahiko Ito[7], Koichi Watashi[1], Mohamed El Kassas[8], Takanobu Kato[1], Asako Murayama[1], Tetsuro Suzuki[7], Kazuaki Chayama[9], Kunitada Shimotohno[10], Masamichi Muramatsu[1#], Hussein H. Aly[1#], Takaji Wakita[1]

Affiliation

[1]Department of Virology II, National Institute of Infectious Diseases, 1-23-1 Toyama, Shinjuku-ku, Tokyo 162-8640, Japan
[2]Department of Microbial Biotechnology, Division of Genetic Engineering and Biotechnology Research, National Research Centre, 33 EL Bohouth St. (formerly El Tahrir St.), Dokki, Giza, P. O. 12622, Egypt
[3]Center for Clinical Sciences, National Center for Global Health and Medicine, 1-21-1 Toyama Shinjuku-ku, Tokyo 162-8655, Japan
[4]Organization for the Strategic Coordination of Research and Intellectual Properties, Meiji University, 1-1-1, Higashi-Mita, Tama-ku, Kawasaki, Kanagawa 214-8571, Japan
[5]Genome Medical Sciences Project, National Center for Global Health and Medicine, 1-7-1 Kohnodai, Ichikawa, Chiba, 272-8516, Japan
[6]Department of Gastroenterology and Metabolism, Graduate School of Biomedical and Health Science, Hiroshima University, 1-2-3 Kasumi, Minami-ku, Hiroshima, 734-8551, Japan
[7]Department of Virology and Parasitology, Hamamatsu University School of Medicine, 1-20-1 Handayama, Higashi-ku, Hamamatsu, Shizuoka, 431-3192, Japan
[8]Endemic Medicine Department, Faculty of Medicine, Helwan University, Cairo, P. O. 11795, Egypt
[9]Collaborative Research Laboratory of Medical Innovation, Graduate School of Biomedical and Health Sciences, Hiroshima University, 1-2-3, Kasumi, Minami-ku, Hiroshima-shi, Hiroshima, 734-8551 Japan
[10]Center for Hepatitis and Immunology, National Center for Global Health and Medicine, Chiba 272-8516, Japan

Corresponding Authors

Hussein H. Aly, email: ahussein@nih.go.jp

Masamichi Muramatsu, email: muramatsu@nih.go.jp

The word count for the abstract: 247 words

The word count for the text: 6191 words

Abstract

Hepatitis B Virus (HBV) is a stealth virus that exhibits only minimal induction of the interferon system that is required for both innate and adaptive immune responses. However, 90% of acutely infected adults can clear the virus, suggesting the presence of additional mechanisms that facilitate viral clearance. Herein, we report that Maf bZIP transcription factor F (MafF) promotes host defense against infection with HBV. Using siRNA library and an HBV/NL reporter virus, we screened to identify anti-HBV host factors. Our data showed that silencing of *MafF* led to a 6-fold increase in luciferase activity after HBV/NL infection. Overexpression of MafF reduced HBV core promoter transcriptional activity, which was relieved upon mutating the putative MafF binding region. Loss of MafF expression by CRISPR/CAS9 (in HepG2-hNTCP-C4 cells) or siRNA silencing (in primary hepatocytes [PXB]), induced HBV core and HBV pregenomic RNA (pgRNA) levels, respectively, after HBV infection. MafF physically binds to HBV core promoter and competitively inhibits HNF-4α binding to an overlapping sequence in HBV enhancer II sequence (EnhII) as seen by ChIP analysis. MafF expression was induced by IL-1β/TNF-α treatment in both HepG2 and PXB cells, in an NF-κB-dependent manner. Consistently, *MafF* expression levels were significantly enhanced and positively correlated with the levels of these cytokines in patients with chronic HBV infection, especially in the immune clearance phase.

63 **Importance**

64 HBV is a leading cause of chronic liver diseases, infecting about 250 million people
65 worldwide. HBV has developed strategies to escape interferon-dependent innate immune
66 responses. Hence, the identification of other anti-HBV mechanisms is important for
67 understanding HBV pathogenesis, and developing anti-HBV strategies. MafF was shown to
68 suppress transcription from HBV core promoter, leading to a significant suppression of HBV
69 life cycle. Furthermore, MafF expression was induced in chronic HBV patients and in
70 primary human hepatocytes (PXB). This induction correlated with the levels of inflammatory
71 cytokines (IL-1β and TNF-α). These data suggest that the induction of MafF contributes to
72 the host's antiviral defense by suppressing transcription from selected viral promoters. Our
73 data shed light on a novel role for MafF as anti-HBV host restriction factor.

74
75
76
77
78
79
80
81
82
83
84
85
86
87
88
89
90

91 **Introduction**

92 In the earliest stages of viral infection, the host initially detects and counteracts
93 infection via induction of innate immune responses (46). Host restriction factors are essential
94 components of the innate antiviral immune response; these factors serve critical roles in
95 limiting virus replication before the adaptive immune response engages to promote virus
96 clearance (5). These antiviral restriction factors are typically induced by cytokines, including
97 interferons (IFNs) (56), transforming growth factor-beta (TGF-β) (29), and interleukin-1-
98 beta (IL-1β) (58). These restriction factors suppress viral replication by targeting the
99 infection at various stages of the virus life cycle, including viral entry (3), transcription of the
100 viral genome (67), viral RNA stability (2), translation of viral proteins (33), viral DNA
101 replication (34), and production of viral particles (6).

102 Approximately 250 million people worldwide are chronically infected with Hepatitis
103 B virus (HBV). These patients are at high risk of developing life-threatening complications,
104 including hepatic cirrhosis, hepatic failure, and hepatocellular carcinoma. Current treatments
105 include nucleos(t)ide analogs that efficiently suppress HBV replication. However, an HBV
106 replication intermediate, covalently closed circular DNA (cccDNA), persists in the nucleus.
107 The cccDNA intermediate gives rise to progeny virus, and may lead to the development of
108 drug-resistant mutants and/or relapsing HBV after drug withdrawal (43). As such, new
109 strategies for HBV treatment are needed.

110 HBV has been identified in human remains from ~7000 years ago (27). This
111 prolonged history and evolution has shaped HBV to be one of the most successful of the
112 "stealth" viruses that can successfully establish infection while evading IFN induction (66).
113 Although HBV can evade IFN induction, the majority of HBV-infected adults (90%) are
114 ultimately able to clear the virus. This observation suggests that there are likely to be one or
115 more IFN-independent host restriction factors that facilitate HBV clearance.

116 The small Maf proteins (sMafs) are a family of basic-region leucine zipper (bZIP)-
117 type transcription factors. MafF, MafG and MafK are the three sMafs identified in vertebrate
118 species (24). sMafs lack a transcriptional activation domain hence, they can act as both
119 transcription activator or repressor based on their expression levels and dimerization partners

120 (19). Intriguingly, previous reports have documented induction of MafF in myometrial cells
121 by inflammatory cytokines, including IL-1β and tumor necrosis factor alpha (TNF-α) (32).
122 However, there have been no previous studies that have addressed a role for MafF in
123 promoting an antiviral innate immune response.

124 Using an HBV reporter virus and an siRNA library, we performed functional siRNA
125 screening to identify the host factors that influence the HBV life cycle. Based on the results
126 of this screen, we identified MafF as a negative regulator of HBV infection. Further analysis
127 revealed that MafF functions as a repressor of transcription at the HBV core promoter,
128 thereby suppressing HBV replication. This is the first study to report a role for MafF as an
129 anti-HBV host factor that represses transcription from the promoters of susceptible viruses.
130
131
132
133
134
135
136
137
138
139
140
141
142
143
144
145
146
147
148

149 **Results**

150

151 **1. MafF suppresses expression of the HBV/NanoLuc (NL) reporter virus**

152 HBV particles carrying a chimeric HBV virus encoding NanoLuc (NL) were prepared as
153 previously described (45). Since these particles carry a chimeric HBV genome in which HBc
154 is replaced by NL, the NL levels released after infection with these particles can only detect
155 the early stages of HBV infection from entry to transcription of HBV-pgRNA (45). We used
156 this high-throughput system, in combination with druggable genome siRNA Library, to
157 screen for host factors that influence these early stages. This approach facilitated testing of
158 2200 human genes for their influence on the HBV life cycle. Screening was performed in
159 HepG2-C4 cells that express the HBV entry receptor, hNTCP (17). Non-targeting siRNAs,
160 and siRNAs against h*NTCP*, were used as controls for each plate (Fig. 1A). Cellular viability
161 was determined using the XTT assay; wells with ≥20% loss of cell viability were excluded
162 from further evaluation. NL activity was induced more than 5 folds (average of 3 different
163 siRNAs) upon the independent silencing of only 10 out of the 2200 host genes (0.4%). These
164 genes were identified as anti-HBV host factors, and based on the induction level of NL
165 activity, these genes were classified into 3 groups: Genes in which NL activity ranged from
166 5 to 10 folds (n=6 genes, MafF fits in this group), from 10 to 20 folds (3 genes), and from 20
167 to 30 folds induction of NL activity (1 gene) (Fig. 1A). MafF was one of the anti-HBV host
168 factors identified by this screening. MafF was previously reported to be induced by famous
169 inflammatory cytokines (IL-1β, and TNF-α), one of the common criteria of anti-viral host
170 restriction factors (29, 56, 58), hence we decided to analyze its role on HBV life cycle.
171 Silencing of *MafF* expression with si-1 or si-3 resulted in 6- ($p < 0.0001$) or 10-fold ($p <$
172 0.001) increases in NL activity, respectively, compared to that observed in cells transfected
173 with the control siRNA (Fig. 1B). The MafF-specific sequence, si-2, did not show a similar
174 effect on NL activity (Fig. 1B). This result was consistent with the fact that si-2 had a lower
175 silencing efficiency for MafF (Fig. 1C). Since NL activity was measured 10 days after siRNA
176 silencing of *MafF* expression, we measured the MafF protein levels at the designated time in

177 order to confirm the prolonged silencing of *MafF* by si-3 (Fig. 1D). Taken together, these
178 findings suggest that MafF may suppress HBV infection.
179
180 **2. MafF strongly suppresses HBV core promoter activity**
181 The HBV/NL reporter system can be used to detect factors affecting the early steps of the
182 HBV life cycle, from HBV entry through cccDNA formation, transcription and translation
183 of HBV-pgRNA (45). Silencing of *MafF* had no impact on cccDNA levels observed in cells
184 infected with HBV as shown by real-time PCR (Fig. 2A) and by southern blot (Fig. 2B);
185 these results indicated that MafF suppressed the HBV life cycle at stage that was later than
186 that of cccDNA formation. Given that MafF can induce transcriptional suppression (19), we
187 analyzed the impact of MafF on various HBV promoters (core, X, preS1, and preS2) using a
188 reporter system in which firefly luciferase coding sequence was inserted downstream to the
189 corresponding HBV promoter. We found that overexpression of MafF resulted in significant
190 suppression of transcription from the HBV core promoter (approximately 8-fold; $p<0.0001$),
191 and significant, albeit less of an impact on transcription from the HBV-X and preS1
192 promoters (both at approximately 2-fold, $p<0.0001$); overexpression of MafF had no
193 significant impact on transcription from the preS2 promoter (Fig. 2C left panel). Likewise,
194 siRNA silencing of endogenous *MafF* enhanced HBV core promoter activity (Fig. 2C right
195 panel, $p<0.0001$). Since the NanoLuc gene in HBV/NL virus (Fig. 1B) is transcribed from
196 an HBV core promoter (45), the findings presented in Fig. 1 and Fig. 2 collectively suggest
197 that MafF-mediated suppression of HBV is mediated primarily by inhibition of transcription
198 from the core promoter.
199
200 **3. MafF suppresses HBV replication**
201 The HBV core promoter controls the transcription of the longest two HBV RNA transcripts,
202 the precore and pgRNAs. HBeAg is translated from the HBV precore RNA, while translation
203 of HBV-pgRNA generates both the polymerase (Pol) and the capsid subunit; the pgRNA also
204 serves as the template for HBV-DNA reverse transcription (4, 14). As such, we assumed that
205 MafF served to inhibit HBV replication by controlling transcription of the HBV core

206 promoter. In fact, overexpression of MafF resulted in significant suppression of the pgRNA
207 titer of HBV genotypes A (GenBank: AB246338.1) and D (GenBank: V01460.1), as
208 demonstrated by RT-qPCR (Fig. 3A, $p<0.0001$ for each genotype). Overexpression of MafF
209 also suppressed the release of HBeAg as measured by enzyme-linked immunosorbent assay
210 (ELISA) (Fig. 3B, $p<0.0001$), as well as the intracellular accumulation of HBV core protein
211 as detected by immunoblotting (Fig. 3C upper and lower panels; $p<0.05$ by densitometric
212 analysis) and the level of HBV core-associated DNA as revealed by southern blot (Fig. 3D).
213

214 **4. MafF-KO induce HBV core protein levels**

215 To further clarify the significance of MafF on HBV infection, we established CRISP/CAS9
216 MafF-KO HepG2-hNTCP-C4 cells. Out of 11 selected clones, MafF-KO-8 and 11 showed
217 the best KO phenotype (Fig. 4A). Myrcludex-B is a lipopeptide consisting of amino acid
218 residues 2–48 of the pre-S1 region of HBV, and is known to block HBV entry [18], pre-
219 treatment with Myrcludex-B (1 μM) 1 hour before infection was performed to confirm that
220 the detected signals were derived from HBV infection and did not represent non-specific
221 background(12). Both MafF-KO-8 and 11 showed a higher NL secretion after HBV/NL
222 infection when compared to parental HepG2-hNTCP-C4 cells with values ranging from 1.5
223 to 3 folds respectively (Fig. 4B). Accordingly, MafF-KO-11 showed 4 times higher HBc
224 levels after HBV infection (Fig. 4C right and left panels). In comparison to the original
225 HepG2-hNTCP-C4 cells, MafF-KO-11 cells showed similar levels of secreted HBs after
226 HBV infection (Fig. 4D), which can be explained by the major function of MafF as a
227 transcriptional repressor of HBV core promoter with minimal to no effect of PreS1 and PreS2
228 promoters (Fig. 2 B and C).
229

230 **5. MafF binds to the HBV core promoter**

231 MafF is a member of (Maf) family of transcription factors,bZIP-type transcription factors
232 that bind to DNA at Maf recognition elements (MAREs). MAREs were initially defined as a
233 13-bp (TGCTGA(G/C)TCAGCA) or 14-bp (TGCTGA(GC/CG)TCAGCA) elements (22,
234 25). The specificity of this binding sequence is greatly affected by the dimerization partners

235 of MafF; multiple studies have presented findings suggesting heterogeneity within MARE
236 sequences, especially when MafF heterodimerizes with anotherbZIP-type transcription
237 factors (26, 44, 53). We next analyzed the HBV core promoter for putative MafF binding
238 region using the JASPAR database of transcription factor binding sites (55). Toward this end,
239 we identified the sequence 5'-TGGACTCTCAGCG-3' that corresponded to nucleotides (nts)
240 1667 to 1679 of the HBV-C_JPNAT genome (GenBank AB246345.1) in the enhancer 2
241 (EnhII) of the HBV core promoter. This motif shared a similarity to a previously defined Maf
242 responsive element (MARE) (19) and also with the DNA binding site for other cap'n'collar
243 (CNC) family proteins Nrf1, Nrf2, Bach1 (Jaspar matrix profiles, MA0506.1, MA0150.1,
244 and MA0591.1, respectively), andbZIP transcription factors that are reported to
245 heterodimerize with sMafs (Fig. 5A). As such, we evaluated the role of this predicted
246 MafF/bZIP site with respect to HBV core promoter activity. We found that the 9th and 11th
247 nucleotides of the aforementioned predicted MafF binding region, which are A and C,
248 respectively, are highly conserved common residues in the predicted MafF/bZIP binding
249 sequence (Fig. 5A). We disrupted this predicted MafF/bZIP site by introducing 2-point
250 mutations (A1676C and C1678A) into the HBV core promoter (Fig. 5A). Despite a minimal
251 but statistically significant reduction of HBV core promoter activity induced by the
252 introduction of these mutations (Fig. 5B left panel, $p<0.0001$), MafF overexpression
253 suppressed the wild-type (WT) core promoter 2–3 times more than that carrying mutations
254 (A1676C and C1678A) (Fig. 5B right panel, $p<0.0001$). Furthermore, ChIP analysis revealed
255 that there was significantly less physical interaction between MafF and the HBV core
256 promoter with A1676C and C1678A mutations than was observed between MafF and the
257 HBV WT counterparts (Fig. 5C, $p<0.05$ for % of input and $p<0.01$ for fold enrichment).
258 These results confirmed that MafF physically binds to the WT HBV core promoter at the
259 putative MafF/bZIP binding region and thereby suppresses transcription. Interestingly the 5'
260 end of the identified MafF/bZIP binding region in HBV core promoter showed high
261 conservation in all HBV genotypes, including ancient HBVs from the Bronze age to the early
262 modern age (appx. 4,500 - 250 years ago), while 3' end showed a relatively less conservation
263 in HBV genotypes A to E, with more sequence divergence in new world HBV genotypes F,

264 G and H (Fig. 5D). The role of these mutations in the escape from MafF-mediated
265 transcriptional repression in these genotypes needs to be further analyzed.
266

267 **6. MafF is a competitive inhibitor of hepatocyte nuclear factor (HNF)-4α binding to**
268 **HBV EnhII**

269 HNF-4α is a transcription factor that has been previously reported to bind HBV core
270 promoter and to induce its transcriptional activity (31, 52, 69). We found that the predicted
271 MafF/bZIP binding region in the EnhII overlaps at it conserved 5' region with an HNF-
272 4α binding site that is located between nucleotides 1662 to 1674 of the HBV C_JPNAT core
273 promoter (10) (Fig. 6A). This finding suggests the possibility that MafF may compete with
274 HNF-4α at these binding sites within the EnhII region. To examine this possibility, we
275 constructed a deletion mutant of EnhII/Cp (EnhII/CpΔHNF-4α#2) that extends from nt 1591
276 to nt 1750; this construct includes the overlapping binding regions identified for MafF and
277 HNF-4α (i.e., HNF-4α site #1 at nt 1662–1674) but lacks the second HNF-4α binding site
278 (HNF-4α site #2 at nt 1757–1769) as shown in Fig. 6A. We performed a ChIP assay and
279 found that the interaction between HNF-4α and EnhII/CpΔHNF-4α #2 was significantly
280 reduced in the presence of MafF (Fig. 6B, $p<0.01$ for % of input and $p<0.05$ for fold
281 enrichment). Furthermore, MafF had no impact on the expression of HNF-4α (Fig. 6C).
282 Together, these data indicated that MafF interacts directly with the HBV core promoter at the
283 putative binding region and suppresses the transcriptional activity of the HBV core promoter
284 by competitive inhibition of HNF-4α binding at an overlapping site in the EnhII region. This
285 competitive suppression is due to partial overlapping of HNF4-α and the putative MafF
286 binding regions in HBV core promoter and did not affect other host genes like ApoA1 and
287 HNF1A known to be regulated by HNF-4α (37, 63) (Fig. 6D).
288

289 **7. IL-1β and TNF-α-mediated induction of MafF expression *in vitro***

290 Given these findings, we speculated that MafF expression might be induced in hepatocytes
291 in response to HBV infection. Based on a previous report of the induction of MafF by both

292 IL-1β and TNF-α in myometrial cells (32), and the fact that both of these cytokines have
293 been implicated in promoting host defense against HBV, we explored the possibility that
294 MafF might be induced by one or more of these cytokines in our *in vitro* system. As shown
295 in Fig. 7, addition of IL-1β or TNF-α resulted in significant induction of *MafF* mRNA
296 expression in HepG2 cells (Fig. 7A, $p<0.0001$ for each cytokine); MafF protein was also
297 detected at higher levels in HepG2 cells exposed to each of these cytokines (Fig. 7B). NF-
298 κB is a downstream regulatory factor that is shared by the IL-1β and TNF-α signaling
299 pathways. We found that chemical inhibition of NF-κB activity with Bay11-7082 or BMS-
300 3455415 suppressed the induction of *MafF* expression in response to IL-1β (Fig. 7C, D;
301 $p<0.05$ for each of these inhibitors) and to TNF-α (Fig. 7E; $p<0.01$). These findings indicate
302 that the IL-1β and TNF-α–mediated induction of *MafF* expression in hepatocytes is regulated
303 by NF-κB signaling. Since we showed that MafF competes with HNF-4α for its interaction
304 with HBV core promoter (Fig. 6), we hypothesized that this effect can be enhanced by IL-
305 1β. We performed a ChIP assay and found that 3 hours after treatment with IL-1β, the
306 interaction between HNF-4α and EnhII/CpΔHNF-4α #2 was significantly reduced. This
307 effect was partially reversed when *MafF* expression was silenced (Fig. 7F, $p<0.01$ for % of
308 input and fold enrichment). These data mechanistically explain the role of MafF on the
309 suppression of HBV core promoter activity by the inflammatory cytokine IL-1β.
310

311 **8. MafF targets HBV infection in human primary hepatocytes**

312 Loss-of-function experiment in the primary hepatocytes is the ideal experimental platform to
313 analyze the physiological significance of endogenous MafF on the HBV life cycle. We
314 silenced *MafF* expression in human primary hepatocytes (PXB cells) using two independent
315 siRNAs, including si-3, which efficiently targets the *MafF* transcript, and si-2, which was
316 associated with a negligible silencing efficiency (Fig. 1C and Fig. 8A, upper panels) followed
317 by infection with HBV (genotype D). *MafF* silencing in response to si-3 resulted in
318 significant induction of HBV-pgRNA, while administration of si-2 did not yield a similar
319 effect (Fig. 8A, lower panels; $p<0.05$). In all experiments, transcription of pgRNA was

320 inversely associated with expression of *MafF* (Fig. 8B, p=0.008); these findings confirmed
321 the role of endogenous MafF with respect to the regulation of HBV-pgRNA transcription.
322 To confirm our earlier findings documenting induction of *MafF* by IL-1β and TNF-α, we
323 treated PXB cells with both cytokines and observed a significant increase in *MafF* mRNA
324 (Fig. 8C, p<0.05 for each cytokine).
325
326 ***9. MafF* expression is higher in HBV chronically infected patients with a positive**
327 **correlation to *IL-1β* and *TNF-α* expression**
328 To explore a role for MafF in HBV infection in human subjects, we evaluated data from an
329 open database (71), and found that *MafF* was expressed at significantly higher levels in
330 patients with chronic HBV compared to healthy individuals (Fig. 9A, p<0.0001); this was
331 notably the case in patients undergoing immune clearance HBV (Fig. 9B, p<0.0001). This
332 result confirmed the induction of *MafF* expression during active inflammation associated
333 with this infection. This observation was strengthened by the demonstration of positive
334 correlations between the levels of *IL-1β* and *TNF-α* transcripts and those encoding *MafF* in
335 the immune clearance patient subset (Fig. 9C, D). Interestingly, no correlations were
336 observed between *MafF* expression and transcripts encoding IFNs (Fig. 9E, F, G, and H).
337 These data suggest that MafF induction associated with chronic HBV disease was unrelated
338 to induction of IFN signaling pathways.
339
340 **Discussion**
341 The intrinsic or innate immune response is mediated by cellular restriction factors.
342 Many of these factors are induced by cytokines (29, 56, 58) and serve to suppress different
343 stages of the viral life cycle, from entry to virion release (5). Several host restriction factors
344 can suppress transcription from DNA virus promoters (57, 67). In this work, we identified
345 MafF as a new host restriction factor that can inhibit both HBV via transcriptional
346 suppression at targeted viral promoter. MafF significantly suppressed HBV core promoter
347 transcription and consequently HBV-pgRNA, core protein and HBV-DNA levels. MafF-KO
348 cells showed a significant increase of HBV core protein with no effect on HBs levels. This

349 can be explained by the major suppressive effect exhibited by MafF on HBV-core promoter
350 in comparison to minimal/no effect of HBV-PreS1, and PreS2 promotors respectively (Fig.
351 2C.)

352 MafF is a member of the small Maf (sMaf) family of transcription factors, a group
353 that includes MafG (20), MafK, and MafF (9). The sMafs arebZIP-type transcription factors
354 that bind to DNA at Maf recognition elements (MAREs). MAREs were initially defined as a
355 13-bp (TGCTGA(G/C)TCAGCA) or 14-bp (TGCTGA(GC/CG)TCAGCA) elements (22,
356 25). However, multiple studies (26, 44, 53) have presented findings suggesting heterogeneity
357 within MARE sequences especially when sMafs heterodimerize with other bZIP-type
358 transcription factors. Using the JASPAR database for transcription factor binding sites, we
359 identified a sequence extending from nt 1667 to 1679 (TGGACTCTCAGCG) in the EnhII
360 region of HBV as a potential MafF/bZIP binding region. Although we did not identify the
361 dimerization partner of MafF in this study, we hypothesize that MafF binds to this region as
362 a heterodimer with another bZIP transcription factor based on the weak alignment at the 5'
363 region of the identified MafF/bZIP binding site when compared to the palindromic MARE
364 consensus sequence. In fact, sMafs/Bach1 dimers were previously reported to act as
365 transcriptional repressors (60), also Bach1 binding site showed a close similarity to the
366 identified MafF/bZIP binding sequence identified in this study (Fig. 5) highlighting the
367 possibility that heterodimers between Bach1/MafF may be behind the MafF-mediated
368 suppression of transcription from HBV core promoter reported in this study. Further studies
369 need to be done to confirm this hypothesis and to identify the dimerization partner of MafF.

370 Both ChIP and functional analysis confirmed the importance of the interaction
371 between MafF and this specific sequence in HBV core promoter; MafF binding at this core-
372 promoter region results in suppression of the transcriptional activity from HBV core
373 promoter and inhibition of the HBV life cycle. Interestingly, the putative MafF/bZIP binding
374 region in the HBV core promoter showed considerable similarity among several HBV
375 genotypes, especially genotypes A, B, and C and ancient HBVs. Although the origin of the
376 HBV infection in humans is still controversial; Paraskevis et al. reported that genotype C is
377 the oldest of human HBVs (47). Indeed, by analyzing ancient HBVs derived from human

378 skeletons or mummies of the Bronze age to the early modern age (appx. 4,500 - 250 years
379 ago), we observed a considerable sequence similarity between the putative MafF/bZIP
380 binding region in these old sequences and that of genotype C (47). These data suggest that
381 MafF has continuously targeted HBV infection since the HBV infected humans (~ 7,000
382 years ago). On the other hand, mutations at the 3' region of the putative MafF/bZIP binding
383 site are more frequent in new world HBV genotypes E, F, and G, suggesting that some HBV
384 genotypes may acquire mutations to overcome MafF-mediated host restriction; however,
385 whether these mutations help in evading the suppressive function of MafF and its impact on
386 HBV life cycle still needs to be addressed.

387 Transcription driven from HBV core promoter is controlled by two enhancers,
388 enhancer I (EnhI) and EnhII, the latter overlapping with the core promoter (EnhII/Cp);
389 transcription is also modulated by a negative regulatory element (NRE) (48). Liver-enriched
390 transcription factors, including C/EBPα, HNF-4α, HNF3, FTF/LRH-1, and HLF4, can
391 interact with the EnhII/Cp region and thereby enhance the core promoter activity (15, 51).
392 Negative regulation of HBV core promoter mainly takes place at the NRE, which is located
393 immediately upstream of EnhII (38). Our analysis of the EnhII segment revealed an overlap
394 between MafF and one of the HNF-4α binding sites located between nt 1662 to nt 1674. We
395 identified MafF as a novel negative regulator of EnhII activity that acts via competitive
396 inhibition of HNF-4α binding to the HBV core promoter at this site; we present this
397 mechanism as a plausible explanation for MafF-mediated suppression of HBV infection.

398 The expression levels of sMafs serve as strong determinants of their overall function. An
399 excess of sMafs may increase shift the balance toward transcriptional repression (40). As
400 discussed previously, sMafs dimerize with CNC family proteins Nrf1, Nrf2, Nrf3, Bach1,
401 and Bach2 (39). Furthermore, MARE consensus sites include an embedded canonical AP1
402 motif; as such, some Jun and Fos family factors can also heterodimerize with Maf/CNC
403 proteins. Finally, large Maf proteins are also capable of binding at MARE elements (21, 41).
404 Given the large number of possible homo- and heterodimeric combinations of proteins
405 capable of binding to MAREs, transcriptional responses ranging from subtle to robust can be
406 elicited at a single MARE site (41). Our findings revealed that MafF expression is induced

407 by IL-1β and TNF-α in primary hepatocytes (PXBs) and that this induction was mediated by
408 NF-κB, an inducible transcription factor that is a central regulator of immune and
409 inflammatory responses (30). Both IL-1β and TNF-α have been associated with protection
410 against HBV. For example, a polymorphism in the IL-1β–gene has been linked to disease
411 progression in patients with HBV-related hepatitis (35), while TNF-α expression in
412 hepatocytes induced by HBV (11) has been shown to decrease the extent of HBV persistence
413 (68). We detected higher levels of *MafF* expression in patients with chronic HBV, especially
414 among those in the immune clearance group, compared to healthy individuals. Moreover, we
415 have also reported that IL-1β treatment significantly suppressed HNF-4α interaction with
416 EnhII region of HBV core promoter in response to the induction of MafF expression.
417 Correlation studies in patients' data alone are not conclusive; however, the combination
418 between the in vitro suppressive function of MafF and patients data suggests a possibly
419 important role for MafF with respect to the anti-HBV effects of these cytokines in HBV-
420 infected patients.

421 HBV core promoter regulates the expression of HBV precore and pgRNA transcripts.
422 The precore-RNA serves as the template for the translation of HBV precore protein. HBV-
423 pgRNA is translated into two proteins, HBc (the capsid-forming protein) and pol
424 (polymerase); the HBV-pgRNA also serves as a template for HBV-DNA reverse
425 transcription and viral replication (1). MafF inhibits HBV replication via suppressing the
426 production of HBV-pgRNA, thereby limiting the production of the corresponding
427 replication-associated protein (core; Fig. 3). We showed here that HBV-pgRNA titers in
428 HBV-infected PXB were higher in cells subjected to MafF silencing; levels of HBV-pgRNA
429 were inversely correlated with MafF mRNA levels (Fig. 7A and B). These data confirmed
430 the importance of endogenous MafF with respect to the regulation of HBV-pgRNA
431 transcription and viral replication. The HBV precore protein is a well-known suppressor of
432 the anti-HBV immune response (36, 64, 70). As such, suppression of HBV precore protein
433 expression may promote a MafF-mediated recovery of the anti-HBV immune response and
434 enhanced viral clearance.

435 To summarize, the results of this work identified MafF as a novel anti-HBV. *MafF*
436 expression was induced by both IL-1β and TNF-α in primary hepatocytes and also in patients
437 with chronic HBV. Furthermore, MafF was shown to play an important role in the
438 suppression of transcription from the HBV core promoter. Further analysis will be needed in
439 order to determine whether the antiviral function of MafF is effective against other DNA
440 viruses as well as its impact on viral evasion mechanisms.
441

442 ## Materials and Methods

443 **Cell culture, reagents and establishment of MafF-KO cells**

444 All the cells used in this study were maintained in culture at 37°C and 5% CO_2. HepG2,
445 HepG2-hNTCP-C4, MafF-KO HepG2-hNTCP-C4, and HepAD38.7-Tet cell lines were
446 cultured in Dulbecco's modified Eagle's medium/F-12 (DMEM/F-12) GlutaMAX media
447 (Gibco) as previously described (17). Primary human hepatocytes (Phoenixbio; PXB cells)
448 were cultured as previously described (16). HEK 293FT cells were cultured in DMEM
449 (Sigma) as previously described (2). For the establishment of puromycin resistant-MafF-KO
450 cells, HepG2-hNTCP-C4 cells were co-transfected with MafF CRISPR/Cas9 KO Plasmid
451 (h), sc-411785, and MafF HDR Plasmid (h), sc-411785-HDR, according to manufacturer
452 instruction. Puromycin selection was conducted at 3 μg/mL. Loss of MafF expression was
453 confirmed by immunoblotting. Myrcludex-B was kindly provided by Dr. Stephan Urban at
454 University Hospital Heidelberg and was synthesized by CS Bio (Shanghai, China).

455 **Plasmid Vectors and Construction**

456 An HBV genotype D subtype ayw replicon (62) was obtained from Addgene. HBV Ae
457 (genotype A), HBV D_IND60, and HBV C_JPNAT are 1.24 HBV replicons, which were
458 described previously (59). A MafF expression plasmid (pFN21AB8874) was purchased from
459 Promega. To add a C-terminal HaloTag, the MafF-encoding sequence was subcloned into
460 the PC14K HaloTag vector using the Carboxy Flexi system (Promega). The reporter plasmid
461 for the HBV core promoter mutant was generated by introducing two point mutations
462 (A1676C and C1678A) at the putative MafF binding region (Fig. 4A). Briefly, several rounds
463 of PCR amplification were performed using pGL4.10_Ce_xmut as the template; the resulting

464 products were digested with *Hind*III and *EcoR*I and subcloned into restriction-digested
465 pGL4.10 (Promega). The set of primers used in the construction of the mutated core promoter
466 include forward primers 5'-TCGAGGAATTCGGGTACTTTACCACAGGAAC-3' and 5'-
467 CTTGGACTCTCCGAAATGTCAACG-3' and reverse primers 5'-
468 TTGCCAAGCTTGAACATGAGATGATTAGGC-3' and
469 5'-CGTTGACATTTCGGAGAGTCCAAG-3'. The sequence encoding HNF-4α was
470 amplified from FR_HNF4A2 (Addgene; (61)) by PCR using primers including forward
471 primer, 5'-AGCTAGGATCCACCATGCGACTCTCCAAAACC-3' and reverse primer 5'-
472 GAGTCGAATTCTTACTTGTCGTCATCGTCTTTGTAGTCAGCAACTTGCCCAAAG
473 CG-3'. The resulting amplification product was cloned into pCDNA3.1 (Invitrogen) to yield
474 pcDNA3.1-HNF4A-FLAG. The reporter deletion mutant EnhII/CPΔHNF-4α #2 (Fig. 5A)
475 was constructed using pGL4.10_Ce_xmut as the template and a primer set, including forward
476 primer 5'- TCGAGGGTACCGCCTGTAAATAGACCTATTG-3' and reverse primer 5'-
477 CTAACAAGCTTTCCTCCCCCAACTCCTCCC-3'; the amplification product was
478 subcloned into pGL4.10 using *Hind*III and *Kpn*I restriction enzymes. All constructs were
479 validated by DNA sequencing. Plasmid DNAs used in transfection experiments were purified
480 using the Purelink Plasmid Midi Kit (Invitrogen).

481 **siRNA library**

482 A Silencer Select™ Human Druggable Genome siRNA Library V4 (4397922, Thermo), was
483 used for screening of HepG2-hNTCP-C4 cells infected with the HBV/NL reporter virus. The
484 siRNAs were arrayed in a 96-well format; siRNAs targeting the same genes with different
485 target sequences were distributed across three plates (A, B, and C). The following plates from
486 this siRNA library (2200 human genes) were screened: 1-1, 1-2, 1-3, 1-4, 2-1, 2-2, 2-3, 2-4,
487 3-1, 5-4, 6-2, 6-3, 9-2, 11-3, 11-4, 13-3, 15-1, 15-4, 19-1, 22-2, 25-3, 25-4, 26-1, 26-2, and
488 26-3. Cellular viability was determined using the XTT assay (Roche) according to the
489 manufacturer's instructions. Wells with ≥ 20% loss of cell viability were excluded from
490 further evaluation. Protocols for the preparation of HBV/NL and screening were as described
491 previously (45).

492 **DNA and RNA transfection**

493 Plasmid DNA transfection was performed according to the manufacturer's guidelines, using
494 Lipofectamine 3000 (Invitrogen) for HepG2 cells and Lipofectamine 2000 (Invitrogen) for
495 HEK 293FT cells. Reverse siRNA transfection into HepG2-hNTCP-C4 or HepG2 was
496 performed using Lipofectamine RNAiMAX (Thermo Fisher Scientific); forward siRNA
497 transfection was performed in PXB cells only using Lipofectamine RNAiMAX according to
498 the respective manufacturer's guidelines. Silencer Select™ si-*MafF* (si-1, s24372; si-2,
499 s24371; and si-3, s24370), si-*MafK* (s194858), si-*MafG* (s8419), and the negative control
500 siRNA (#2) were purchased from Thermo Fisher Scientific.

501 **Western blot analysis**

502 Cells were lysed with PRO-PREP protein extraction solution (Intron Biotechnology). Protein
503 samples were separated on a 12% gel via SDS-PAGE. Immunoblotting and protein detection
504 were performed as previously reported (2). Primary antibodies included mouse monoclonal
505 anti-HBc (provided by Dr. Akihide Ryo, Yokohama City University), anti-Halo-tag
506 (Promega), anti-FLAG (M2, Sigma), and anti-actin (Sigma), rabbit polyclonal anti-MafF
507 (Protein Tech), and rabbit monoclonal anti-HNF-4α (Abcam). The band intensities were
508 quantified by ImageJ software (NIH).

509 **HBV and HBV/NL preparation and infection**

510 HBV particles carrying a chimeric HBV virus encoding NanoLuc (NL) were prepared and
511 used as described previously (45). Briefly, HepG2 cells were transfected with a plasmid
512 encoding HBV in which the core region was replaced by a gene encoding NL and a helper
513 plasmid that carried an HBV genome that was defective in packaging. The resulting HBV/NL
514 particles produced NL upon infection. HBV and HBV/NL stocks used in this study were
515 prepared as described previously (17, 45) For infection of HepG2-hNTCP-C4 cells, the cells
516 first were reverse-transfected with *MafF* or negative control siRNAs two days prior to the
517 HBV infection and then infected 2 days later with inoculation of HBV or HBV/NL as
518 described previously (17, 45); the experiment was terminated at 8 days post-infection. For
519 PXB cells, the cells were first infected with HBV; at 3 days post-infection, the cells were
520 transfected with the siRNAs, and the experiment was terminated at 7 days post-infection.

521 **RNA extraction and quantitative real-time PCR**

522 Isolation of total cellular RNA was performed with a RNeasy Mini kit (Qiagen) according to
523 the manufacturer's guidelines and cDNA synthesis was performed using a Superscript VILO
524 cDNA Synthesis Kit (Thermo Fisher Scientific). The relative levels of the *MafF* mRNA was
525 determined using TaqMan 746 Gene Expression Assay primer-probe sets (Applied
526 Biosystems) Hs05026540_g1, expression of *ACTB* (primer-probe set 748 Hs99999903_m1)
527 was used as an internal control for normalization. The quantification of pgRNA, *NTCP*,
528 *HNF-4α, APOA1, and HNF1A* was performed using Power SYBR Green PCR Master Mix
529 (Applied Biosystems); for these transcripts, expression of *GAPDH* was used as an internal
530 control for normalization. Data were expressed as fold change relative to the mean of the
531 control group. The set of primers used in these assays included the Precore forward primer
532 5'-ACTGTTCAAGCCTCCAAGCTGT-3' and reverse primer 5'-
533 GAAGGCAAAAACGAGAGTAACTCCAC-3', *NTCP* forward primer 5′-
534 AGGGAGGAGGTGGCAATCAAGAGTGG-3' and reverse primer 5'-
535 CCGGCTGAAGAACATTGAGGCACTGG-3', *HNF-4α* forward primer 5'-
536 ACTACGGTGCCTCGAGCTGT-3' and reverse primer 5'-
537 GGCACTGGTTCCTCTTGTCT-3'; APOA1 forward primer 5'-
538 CCTTGGGAAAACAGCTAAACC-3', APOA1 reverse primer 5'-
539 CCAGAACTCCTGGGTCACA-3', HNF1A forward primer 5'-
540 CCATCCTCAAAGAGCTGGAG-3', HNF1A reverse primer 5'-
541 TGTTGTGCTGCTGCAGGTA-3', *GAPDH* forward primer 5'-CTTTTGCGTCGCCAG-3'
542 and reverse primer 5'-TTGATGGCAACAATATCCAC-3'.

543 **DNA extraction and cccDNA quantification**

544 For selective extraction of cccDNAs for quantitative PCR, HBV-infected HepG2-hNTCP-
545 C4 cells were harvested and total DNA was extracted using a Qiagen DNA extraction kit
546 according to the manufacturer's instructions but without the addition of Proteinase K as
547 recommended by the concerted harmonization efforts for HBV cccDNA quantification
548 reported in the 2019 International HBV meeting (28). Levels of cccDNA were measured by
549 quantitative real-time PCR (qPCR) using the TaqMan Gene Expression Master Mix (Applied
550 Biosystems), specific primers, and probe as described previously (50). Data were processed

551 as $2^{(-\Delta\Delta Ct)}$ for quantification of cccDNA using chromosomal *GAPDH* DNA sequence (via
552 primer-probe set Hs04420697_g1; Applied Biosystems) as an internal normalization control.

553 **Dual luciferase reporter assay**

554 Firefly luciferase reporter plasmids carrying the entire HBV core promoter (nt 900 to 1817),
555 Enh1/X promoter (nt 950 to 1373), preS1 promoter (nt 2707 to 2847), or preS2/S promoter
556 (nt 2937 to 3204) were constructed as previously reported (8). HepG2 cells were co-
557 transfected with the firefly reporter vectors and the *Renilla* luciferase plasmid pRL-TK
558 (Promega) as an internal control. At 48 h post-transfection, the cells were lysed and luciferase
559 activities were measured using the Dual-Luciferase Reporter Assay System (Promega). For
560 experiments involving IL-1β, cells were treated for 3 h with IL-1β (1 ng/ml) at 48 h post-
561 transfection followed by evaluation of dual luciferase activity.
562

563 **Quantification of HBs and HBe antigens**

564 Cell supernatants were harvested and an ELISA was performed as described previously for
565 HBs (65) whereas for HBe, Enzygnost HBe monoclonal, Siemens was used according to the
566 manufacturer's instructions.
567

568 **Indirect Immunofluorescence Analysis**

569 Indirect immunofluorescence analysis was performed essentially as described previously
570 (65). After fixation with 4% paraformaldehyde and permeabilization with 0.3% Triton X-
571 100, an anti-HBc antibody (HBP-023-9, Austral Biologicals) was used as the primary
572 antibody.

573 **Southern blotting assay**

574 HepG2 cells were co-transfected with MafF-encoding or control vectors together with the
575 HBV ayw plasmid both with or without 5 μM entecavir (Sigma) as a control. At 3 days post-
576 transfection, core-associated DNA was isolated from intracellular viral capsids as described
577 previously (54). Southern blot analysis to detect HBV-DNAs was performed also as
578 described previously (2) For the detection of HBV cccDNA by southern blotting, the HBV

579 cccDNA was extracted through protein free Hirt DNA extraction. Hirt DNA was heated at
580 95ºC for 10 minutes to allow the denaturation of DP-rcDNA and dsDNA into single stranded
581 DNA. The heat-treated samples were then digested with EcoRI to linearize the cccDNA. The
582 Hirt DNA samples were then separated by agarose gel at 25 volts for 12 hours. After southern
583 blot transfer, the DNA was hybridized with DIG Easy Hyb (Roche-11603558001) and
584 detected with DIG wash and block buffer set (Roche-11585762001).

585 **Chromatin Immunoprecipitation (ChIP) assay**

586 293FT cells were co-transfected with a MafF expression plasmid together a reporter plasmid
587 harboring either the WT or mutated core promoter (substitution mutations in MARE) at a 4:1
588 ratio for assessment of the interactions between MafF and HBV core promoter. In other
589 experiments, 293FT cells were co-transfected with plasmids encoding FLAG-tagged
590 EnhII/CPΔHNF-4α#2, and a MafF expression plasmid (or empty vector) at a 1: 2 ratio for
591 assessment of competitive binding of MafF and HNF-4α. Rabbit monoclonal anti-HNF-4α
592 (Abcam, EPR16885) was used for IP. To elucidate the effect of IL-1β on MafF and HNF-4α
593 competition, HepG2 cells were transfected with anti-MafF si-3 and plasmid encoding
594 EnhII/CPΔHNF-4α#2. At 48 h post-transfection IL-1β was added to the culture medium
595 (1ng/mL) for 3 hours. ChIP was carried out using a Magna ChIP G kit (Millipore) according
596 to the manufacturer's instructions. Anti-HNF-4α Rabbit monoclonal antibody (Abcam) was
597 used for IP.

598

599 **Cytokine treatment and NF-κB inhibitors**

600 Responses to IL-1β and TNF-α (R&D Systems) were evaluated in HepG2 cells (at 1 ng/ml
601 and 10 ng/ml, respectively) and in PXB cells (both at 10 ng/ml) after 1, 3, and 6 h. For the
602 experiments involving NF-κB inhibitors, Bay11-7082 and BMS-345541 (both from Tocris)
603 were added to final concentrations of 10 μM and 5 μM, respectively. HepG2 cells were
604 pretreated for 1 h with each inhibitor followed by the addition of 1 ng/ml IL-1β (for 1 and 3
605 h) or 10 ng/ml TNF-α (for 1 h). All experiments included phosphate-buffered saline (PBS)
606 as a diluent control for the cytokines and dimethyl sulfoxide (DMSO) as the diluent control
607 for the NF-κB inhibitors.

608

609 **Database**

610 Transcriptional profiling of the patients with chronic HBV (CHB) (GSE83148) and of HBV
611 patients with immune tolerance and those undergoing HBV clearance (GSE65359) were
612 identified in the Gene Expression Omnibus public database. Expression data for *MafF* and
613 for genes encoding cytokines *IL-1β, TNF-α, IFNA1, IFN-β1, IFNL1, and IFNL2* were
614 extracted by GEO2R. HBx sequences (n = 10,846) were collected from HBVdb (13) , and 13
615 ancient HBV sequences were downloaded from the NCBI nucleotide database (18, 42, 49).
616 For each genotype, nucleotide sequences were aligned by using MAFFT version 7.471 (23).
617 Multiple sequence alignments of the MARE region were depicted using WebLogo version
618 2.8 (7). The overall height of the stack indicates the conservation at the site while the relative
619 frequency of each nucleic acid is shown as the height of the characters within the stack.

620 **Statistical analysis**

621 The data were analyzed with algorithms included in Prism (v. 5.01; GraphPad Software, San
622 Diego, CA). Tests for normal distribution of the data were performed. Two-tailed unpaired t
623 tests, and Mann-Whitney U tests were used for statistical analysis of parametric and non-
624 parametric data, respectively. The correlation coefficients were determined by Pearson or
625 Spearman correlation analysis of parametric and non-parametric data, respectively. Values
626 of $p \leq 0.05$ were considered statistically significant.

627

628 **<u>Acknowledgments</u>**

629 Ibrahim MK was the recipient of a JSPS postdoctoral fellowship. This study was supported
630 by a Grant-In-Aid for JSPS Fellows (18F18098), and for Scientific Research (19K07586),
631 and grants from the Research Program on Hepatitis from the Japan Agency for Medical
632 Research and Development (AMED; 19fk0310104j0903, 19fk0310103j0303,
633 19fk0310109h0003, and 19fk0310109j0403). Myrcludex-B, a pre-S1 lipopeptide, was kindly
634 provided by Dr. Stephan Urban at the University Hospital Heidelberg. We gratefully
635 acknowledge Dr. Akihide Ryo (Yokohama City University School of Medicine) for the kind
636 gift of the anti-HBV core antibody, Dr. Takayuki Murata (Fujita Health University), Dr. Iwao

637 Kukimoto, Miss Yingfang Li, Dr. Xin Zheng, and Dr. Haruka Kudo (NIID) for productive
638 discussion, criticism, and technical support. We are also very grateful to Dr. Haitao Guo
639 (University of Pittsburgh) for his great support that enabled us to detect HBV-cccDNA by
640 southern blot assay.
641

642 ## Figure Legends

643 **Figure 1. MafF suppresses HBV infection**

644 **A.** A schematic diagram showing the experimental approach used to screen the siRNA library.
645 **B.** HepG2-hNTCP-C4 cells were transfected with control, *NTCP*, or *MafF*-targeting siRNAs
646 (si-1, si-2, and si-3); two days later, transfected cells were infected with the HBV/NL reporter
647 virus. At day 8 post-infection, luciferase assays were performed, and NanoLuc activity was
648 measured and plotted. **C.** HepG2 cells were transfected with control or *MafF*-targeting
649 siRNAs (si-1, si-2, and si-3); total protein was extracted after two days. Expression of MafF
650 (upper panel) and actin (control; lower panel) was analyzed by immunoblotting with their
651 respective antibodies. **D.** HepG2 cells were transfected with control or *MafF*-targeting siRNA
652 (si-3); total protein was extracted after ten days. Expression of MafF (upper panel) and actin
653 (control; lower panel) was analyzed by immunoblotting with their respective antibodies. All
654 assays were performed in triplicate and included three independent experiments. Data are
655 presented as mean±standard deviation (SD); $^{**}p<0.01$, $^{***}p<0.001$, $^{****}p< 0.0001$; NS, not
656 significant
657

658 **Figure 2. MafF suppresses the transcriptional activity of the HBV core promoter.**

659 **A.** HepG2-hNTCP-C4 cells were transfected with control or *MafF*-targeting siRNA (si-3).
660 Two days after transfection, the transfected cells were infected with HBV at 12,000 genomic
661 equivalents (GEq) per cell. Eight days later, the cells were harvested, DNA was extracted,
662 and cccDNA was quantified by real-time PCR. The data were normalized to the levels of
663 endogenous *GAPDH DNA* and are presented as fold change relative to control siRNA-
664 transfected cells. **B.** HepG2-hNTCP-C4 cells were transfected with control or *MafF*-targeting
665 siRNA (si-3). Two days after transfection, the transfected cells were infected with HBV at

666 12,000 GEq per cell. Eight days later, the cells were harvested, HIRT purification of DNA
667 was performed, and cccDNA was visualized by southern blotting assay. **C.** HepG2 cells (left
668 panel) were co-transfected with a MafF expression vector or empty vector (control) together
669 with firefly luciferase reporter plasmids with HBV promoters (core, X, S1, and S2) and the
670 pRL-TK control plasmid encoding *Renilla* luciferase. Two days after transfection, the cells
671 were harvested and evaluated by dual luciferase assay. HepG2 cells (right panel) were
672 transfected with control or *MafF*-targeting siRNA (si-3); 24 hours later, the cells were
673 transfected with firefly luciferase reporter-HBV core promoter vector and the pRL-TK
674 plasmid encoding *Renilla* luciferase. Two days later, the cells were lysed and evaluated by
675 dual luciferase assay. For panel C, firefly luciferase data were normalized to *Renilla*
676 luciferase levels; relative light units (RLUs) for firefly luciferase were plotted as fold
677 differences relative to the levels detected in the control groups. All assays were performed in
678 triplicate and included three independent experiments; data are presented as mean±SD.
679 ****p<0.0001; NS, not significant.
680
681 **Figure 3. MafF suppresses HBV life cycle.**
682 **A.** HepG2 cells were transfected with empty (control) or MafF expression vector together
683 with expression vectors encoding HBV genotypes A and D. Two days later, the cells were
684 harvested and the pgRNA expression was quantified by real-time RT-PCR. The data were
685 normalized to the expression of *GAPDH* and are shown as the fold change relative to control
686 plasmid-transfected cells. **B–D:** HepG2 cells were transfected with empty (control) or MafF
687 expression vectors together with an expression plasmid encoding HBV genotype D **(B)** At 2
688 days post-transfection, HBeAg in the cell culture supernatants were quantified by ELISA.
689 **(C)** The intracellular levels of HBV core protein (upper left panel) and actin (loading control;
690 lower left panel) were evaluated by immunoblotting; the intensities of the bands (right panel)
691 were quantified by ImageJ software. **(D)** At 3 days post-transfection, the levels of
692 intracellular core-associated DNA were determined by southern analysis; transfected cells
693 treated with 10 μM entecavir were used as controls.

694 Data are presented as fold differences relative to the control plasmid-transfected cells. All
695 assays were performed in triplicate and include results from three independent experiments;
696 data are presented as mean±SD; *p<0.05, ****p<0.0001.
697
698 **Fig. 4. Enhanced expression of HBc in MafF-KO cells.**
699 A. HepG2-hNTCP-C4 cells were co-transfected with MAfF CRISPR/Cas9 KO Plasmid (h),
700 sc-411785, and MAfF HDR Plasmid (h), sc-411785-HDR. Puromycin selection was
701 conducted at 3μg/mL for 2 weeks. 11 isolated colonies were picked and scaled up. MafF
702 expression was detected by immunoblotting, as positive and negative controls, we used WT
703 (HepG2-hNTCP-C4) cells, and si-3 treated HepG2-hNTCP-C4 cells respectively. B. HepG2-
704 hNTCP-C4, MafF-KO-8, and MafF-KO-11 cells were infected with HBV/NL reporter virus.
705 Cells were pretreated with or without 1 μM Myrcludex-B or vehicle (DMSO) for 3 h before
706 infection. At day 8 post-infection, luciferase assays were performed, and NanoLuc activity
707 was measured and plotted as fold-difference relative to the mean luciferase levels in HepG2-
708 hNTCP-C4 cells. C. HepG2-hNTCP-C4, or MafF-KO-11 cells were infected with HBV
709 (6000 GEq/cell), at 12 days post-infection, HBc in the cells was detected by
710 immunofluorescent (left panel) and fluorescent intensity was plotted as fold-difference
711 relative to its mean levels in HBV-infected HepG2-hNTCP-C4 cells. D. HepG2-hNTCP-C4,
712 or MafF-KO-11 cells were infected with HBV (6000 GEq/cell). Cells were pretreated with
713 or without 1 μM Myrcludex-B or vehicle (DMSO) for 3 h before infection. After 12 days from
714 infection, HBsAg in the cell culture supernatants was measured and plotted as fold-difference
715 relative to the its mean levels in the supernatant of HBV-infected HepG2-hNTCP-C4 cells.
716 All assays were performed in triplicate and include results from three independent
717 experiments; data are presented as mean±SD; **p<0.01, ***p<0.001.
718
719
720 **Figure 5. Physical interaction of MafF with HBV core promoter is required for**
721 **transcriptional repression.**

722 **A.** A schematic representation of the putative MafF/bZIP binding region within enhancer 2
723 (EnhII) of the HBV core promoter from HBV genotype C. A mutant construct was prepared
724 by introducing two point mutations (A1676C and C1678A) into the MARE sequence
725 identified in the wild-type (WT) core promoter. **B.** HepG2 cells were co-transfected with
726 mock (left panel) or a MafF expression plasmid (right panel) along with an HBV core
727 promoter (WT or mutant)-reporter plasmid and pRL-TK encoding *Renilla* luciferase. At two
728 days post-transfection, a dual luciferase assay was performed; firefly luciferase data were
729 normalized relative to *Renilla* luciferase levels, and RLUs for firefly luciferase are plotted as
730 fold differences relative to activity in the control group. **C.** 293FT cells were transfected with
731 either the WT or mutant HBV core promoter-luciferase reporter plasmid together with a
732 MafF expression plasmid (at a ratio 1:4). At two days post-transfection, cell lysates were
733 collected; two aliquots (1/10 volume each) were removed from each sample. One aliquot was
734 used for the detection of MafF protein (Input) and actin (loading control) by immunoblotting
735 (right upper and middle panels); the second aliquot was used for DNA extraction and
736 detection of HBV core promoter (Input) by real-time PCR. The remaining cell lysates (each
737 8/10 of the original volume) were subjected to ChIP assay using either isotype control
738 antibody (rabbit IgG) or rabbit anti-MafF IgG to detect MafF. Following
739 immunoprecipitation (IP), 1/10 volume of each IP sample was analyzed by immunoblotting
740 for MafF (right lower panel); each remaining IP sample was subjected to DNA extraction
741 and real-time PCR assay in order to detect associated HBV core promoter DNA. The fraction
742 of core promoter DNA immunoprecipitated compared to the input value was determined by
743 real-time PCR and was expressed as percent of input (% of input) and as the fold enrichment
744 over the fraction of *GAPDH* DNA immunoprecipitated. D. A schematic representation of the
745 putative MafF/bZIP binding region within enhancer 2 (EnhII) of the HBV core promoter
746 from different HBV genotypes. 10,846 HBx sequences were collected from HBVdb, The
747 multiple sequence alignments of the MARE region were depicted by using WebLogo version
748 2.8. The overall height of the stack indicates the conservation at the site, while the relative
749 frequency of each nucleic acid is shown as the height of the characters within the stack. The

750 assays of panel B and C were performed in triplicate and include data from three independent
751 experiments. Data are presented as mean±SD; *p<0.05, **p<0.01, ****p<0.0001.
752
753 **Figure 6. MafF competes with HNF-4α for binding to the HBV core promoter.**
754 **A.** A schematic representation of the enhancer 2 (EnhII) and the basal HBV core promoter
755 (Cp; nt 1591-1798) featuring the putative MafF binding region (nt 1667–1679) and the two
756 HNF-4α binding sites HNF-4α#1 (nt 1662–1674) and HNF-4α#2 (nt 1757–1769). A deletion
757 mutant construct (EnhII/Cp Δ HNF-4α#2, nt 1591–1750) was prepared to eliminate HNF-
758 4α#2. **B.** 293FT cells were co-transfected with the EnhII/Cp Δ HNF-4α#2-luciferase reporter
759 plasmid, a FLAG-tagged HNF-4α expression plasmid, and a MafF (or control) expression
760 plasmid at a ratio of 1:1:2. At two days post-transfection, cell lysates were collected and two
761 aliquots (1/10 volume each) were removed from each sample. One aliquot was used for the
762 detection of HNF-4α protein (Input) and actin (loading control) by immunoblotting (lower
763 panel); the second aliquot was used for DNA extraction and detection of HBV core promoter
764 (Input) by real-time PCR. The remaining cell lysates (each 4/10 of the original volume) were
765 subjected to ChIP assay using isotype control antibody (rabbit IgG) or rabbit anti-HNF-4α
766 IgG to precipitate FLAG-tagged HNF-4α. Following immunoprecipitation (IP), 1/5 volume
767 of each IP sample was analyzed by immunoblotting to detect HNF-4α (lower panel) and each
768 remaining IP sample was subjected to DNA extraction and real-time PCR assay for the
769 detection of associated HBV core promoter DNA. The fraction of core promoter DNA
770 immunoprecipitated compared to the input value was determined by real-time PCR and was
771 expressed as percent of input (% of input) (upper left panel) and as the fold enrichment (upper
772 right panel) over the fraction of *GAPDH* DNA immunoprecipitated. **C. Left panel:** HepG2
773 cells were transfected with empty vector (control) or MafF expression vector. After 24 h or
774 48 h, total RNA was extracted and *HNF-4α* expression was quantified by real-time RT-PCR.
775 The data were normalized to *GAPDH* expression and are presented as fold differences
776 relative to the control cells. **Right panel:** HepG2 cells were transfected with control or *MafF*-
777 targeting siRNA (si-3) and *HNF-4α* expression was evaluated 48 h later as noted just above.

778 **D.** HepG2 cells were transfected with control or *MafF*-targeting siRNA (si-3), and *HNF1A*
779 and *ApoA-1* expression was evaluated after 48 h as previously mentioned . All assays were
780 performed in triplicate and data are presented from three independent experiments. Data are
781 presented as mean±SD; *p<0.05, **p<0.01; NS, not significant.
782
783 **Figure 7. IL-1β and TNF-α induce MafF expression via NF-κB-mediated signaling**
784 **A.** HepG2 cells were treated with IL-1β (1 ng/ml), TNF-α (10 ng/ml), or PBS (diluent
785 control) for the times as indicated (hours). The cells then were lysed, total cellular RNA was
786 extracted, and *MafF* mRNA was quantified by real-time RT-PCR. The data were normalized
787 to the expression of *ACTB* and are shown as the fold change relative to the mean of the control
788 group. **B.** HepG2 cells were treated for 24 h with IL-1β, TNF-α, or PBS control as in A.; the
789 cells then were harvested and total protein was extracted. Expression of MafF (upper panel)
790 and actin (the loading control; lower panel) was analyzed by immunoblotting. **C, D, and E.**
791 HepG2 cells were pretreated with NF-κB inhibitors Bay11-7082**,** BMS-345541, or DMSO
792 (diluent control) for 1 h and then treated with 1 ng/ml IL-1β (**C, D**), 10 ng TNF-α (**E**) or PBS
793 (control) for 1 and 3 h. Expression of MafF was quantified by real-time RT-PCR and were
794 normalized to the expression of the *ACTB* and shown as the fold change relative to the mean
795 of the control group. **F.** HepG2 cells were transfected with the anti-MafF si-3 and EnhII/Cp
796 ΔHNF-4α#2-luciferase reporter plasmid. At two days post-transfection, cells were treated
797 with IL-1β (1 ng/mL) or mock for 3 hours, then cell lysates were collected and two aliquots
798 (1/10 volume each) were removed from each sample. One aliquot was used for the detection
799 of HNF-4α protein (Input) and actin (loading control) by immunoblotting (lower panel); the
800 second aliquot was used for DNA extraction and detection of HBV core promoter (Input) by
801 real-time PCR. The remaining cell lysates (each 4/10 of the original volume) were subjected
802 to ChIP assay using isotype control antibody (rabbit IgG) or rabbit anti-HNF-4α IgG to
803 precipitate endogenous HNF-4α. Following immunoprecipitation (IP), 1/5 volume of each IP
804 sample was analyzed by immunoblotting to detect HNF-4α (lower panel) and each remaining
805 IP sample was subjected to DNA extraction and real-time PCR assay for the detection of

806 associated EnhII/Cp Δ HNF-4α#2 DNA. The fraction of EnhII/Cp Δ HNF-4α#2 DNA
807 immunoprecipitated compared to the input value was determined by real-time PCR and was
808 expressed as percent of input (% of input) (upper left panel) and as the fold enrichment (upper
809 right panel) over the fraction of *GAPDH* DNA immunoprecipitated.
810 All assays were performed in triplicate and including the results from three (panels A, B, and
811 C) or two (D, E and F) independent experiments. Data are presented as mean±SD; *p<0.05,
812 ***p*<0.01, ****p*<0.001, *****p*< 0.0001.
813
814 **Figure 8. MafF suppresses HBV infection in primary human hepatocytes (PXB cells).**
815 **A.** Primary hepatocytes (PXB cells) were infected with HBV virions at 5,000 GEq per cell.
816 After 3 days, the cells were transfected with control or *MafF*-targeting siRNAs (si-2 and si-
817 3); at 4 days after transfection, total RNA was extracted. **Upper panel:** *MafF* expression
818 level was quantified by real-time RT-PCR and normalized to the expression of *ACTB*. **Lower**
819 **panel:** Levels of pgRNA were quantified by real-time RT-PCR using a standard curve
820 quantification method. Data are presented as fold differences relative to the control siRNA-
821 transfected cells. **B.** Correlation between expression of *MafF* mRNA and pgRNA in HBV-
822 infected and siRNA-transfected PXB cells as described in A. **C.** Primary hepatocytes (PXB)
823 cells were treated with IL-1β (at 10 ng/ml), TNF-α (at 10 ng/ml), or PBS (diluent control) for
824 the times indicated (hours). The cells then were lysed, total cellular RNA was extracted, and
825 *MafF* mRNA was quantified by real-time RT-PCR. The data were normalized to the
826 expression of *ACTB* and are shown as the fold change relative to the mean of the control
827 group. D. MafF mRNA expression detected by RNA sequencing in single primary hepatocyte
828 (PXB) infected with HBV. All assays were performed in triplicate and include data from two
829 independent experiments. Data are presented as mean±SD; **p*<0.05, ***p*<0.01; NS, not
830 significant
831
832 **Figure 9. *MafF* expression is increased in patients with chronic HBV infections and is**
833 **positively correlated to expression of *IL-1β* and *TNF-α* mRNAs**

834 **A.** *MafF* mRNA levels in the liver tissue of patients with chronic hepatitis B infection (CHB;
835 n=122) and healthy subjects (n=6, GSE83148). **B.** *MafF* mRNA levels in the liver tissue of
836 immune-tolerant (n=22) and immune clearance (n=50) HBV-infected patients (GSE65359).
837 **C.-H.** Correlations between the expression of mRNAs encoding *MafF* and **C.** *IL-1β*, **D.** *TNF-*
838 *α*, **E**. *IFN-β1*, **F.** *IFNA1*, **G**. *IFNL1*, and **H**. *IFNL2* in liver tissue of patients undergoing
839 immune clearance. In panels A and D, data are presented as the mean±SD; ****p<0.0001.
840
841
842 **References**
843

844 1. **Abraham, T. M., and D. D. Loeb.** 2007. The topology of hepatitis B virus pregenomic RNA
845 promotes its replication. J Virol **81:**11577-84.
846 2. **Aly, H. H., J. Suzuki, K. Watashi, K. Chayama, S. Hoshino, M. Hijikata, T. Kato, and T. Wakita.**
847 2016. RNA Exosome Complex Regulates Stability of the Hepatitis B Virus X-mRNA Transcript
848 in a Non-stop-mediated (NSD) RNA Quality Control Mechanism. J Biol Chem **291:**15958-74.
849 3. **Amini-Bavil-Olyaee, S., Y. J. Choi, J. H. Lee, M. Shi, I. C. Huang, M. Farzan, and J. U. Jung.**
850 2013. The antiviral effector IFITM3 disrupts intracellular cholesterol homeostasis to block
851 viral entry. Cell Host Microbe **13:**452-64.
852 4. **Bartenschlager, R., and H. Schaller.** 1992. Hepadnaviral assembly is initiated by polymerase
853 binding to the encapsidation signal in the viral RNA genome. EMBO J **11:**3413-20.
854 5. **Chemudupati, M., A. D. Kenney, S. Bonifati, A. Zani, T. M. McMichael, L. Wu, and J. S.**
855 **Yount.** 2019. From APOBEC to ZAP: Diverse mechanisms used by cellular restriction factors
856 to inhibit virus infections. Biochim Biophys Acta Mol Cell Res **1866:**382-394.
857 6. **Chen, G., C. H. Liu, L. Zhou, and R. M. Krug.** 2014. Cellular DDX21 RNA helicase inhibits
858 influenza A virus replication but is counteracted by the viral NS1 protein. Cell Host Microbe
859 **15:**484-93.
860 7. **Crooks, G. E., G. Hon, J. M. Chandonia, and S. E. Brenner.** 2004. WebLogo: a sequence logo
861 generator. Genome Res **14:**1188-90.
862 8. **Deng, L., X. Gan, M. Ito, M. Chen, H. H. Aly, C. Matsui, T. Abe, K. Watashi, T. Wakita, T.**
863 **Suzuki, T. Okamoto, Y. Matsuura, M. Mizokami, I. Shoji, and H. Hotta.** 2019. Peroxiredoxin
864 1, a Novel HBx-Interacting Protein, Interacts with Exosome Component 5 and Negatively
865 Regulates Hepatitis B Virus (HBV) Propagation through Degradation of HBV RNA. J Virol **93**.
866 9. **Fujiwara, K. T., K. Kataoka, and M. Nishizawa.** 1993. Two new members of the maf
867 oncogene family, mafK and mafF, encode nuclear b-Zip proteins lacking putative trans-
868 activator domain. Oncogene **8:**2371-80.
869 10. **Gilbert, S., L. Galarneau, A. Lamontagne, S. Roy, and L. Belanger.** 2000. The hepatitis B virus
870 core promoter is strongly activated by the liver nuclear receptor fetoprotein transcription
871 factor or by ectopically expressed steroidogenic factor 1. J Virol **74:**5032-9.

872 11. **Gonzalez-Amaro, R., C. Garcia-Monzon, L. Garcia-Buey, R. Moreno-Otero, J. L. Alonso, E.**
873 **Yague, J. P. Pivel, M. Lopez-Cabrera, E. Fernandez-Ruiz, and F. Sanchez-Madrid.** 1994.
874 Induction of tumor necrosis factor alpha production by human hepatocytes in chronic viral
875 hepatitis. J Exp Med **179:**841-8.
876 12. **Gripon, P., I. Cannie, and S. Urban.** 2005. Efficient inhibition of hepatitis B virus infection by
877 acylated peptides derived from the large viral surface protein. J Virol **79:**1613-22.
878 13. **Hayer, J., F. Jadeau, G. Deleage, A. Kay, F. Zoulim, and C. Combet.** 2013. HBVdb: a
879 knowledge database for Hepatitis B Virus. Nucleic Acids Res **41:**D566-70.
880 14. **Hirsch, R. C., J. E. Lavine, L. J. Chang, H. E. Varmus, and D. Ganem.** 1990. Polymerase gene
881 products of hepatitis B viruses are required for genomic RNA packaging as wel as for reverse
882 transcription. Nature **344:**552-5.
883 15. **Ishida, H., K. Ueda, K. Ohkawa, Y. Kanazawa, A. Hosui, F. Nakanishi, E. Mita, A. Kasahara,**
884 **Y. Sasaki, M. Hori, and N. Hayashi.** 2000. Identification of multiple transcription factors, HLF,
885 FTF, and E4BP4, controlling hepatitis B virus enhancer II. J Virol **74:**1241-51.
886 16. **Ishida, Y., C. Yamasaki, A. Yanagi, Y. Yoshizane, K. Fujikawa, K. Watashi, H. Abe, T. Wakita,**
887 **C. N. Hayes, K. Chayama, and C. Tateno.** 2015. Novel robust in vitro hepatitis B virus
888 infection model using fresh human hepatocytes isolated from humanized mice. Am J Pathol
889 **185:**1275-85.
890 17. **Iwamoto, M., K. Watashi, S. Tsukuda, H. H. Aly, M. Fukasawa, A. Fujimoto, R. Suzuki, H.**
891 **Aizaki, T. Ito, O. Koiwai, H. Kusuhara, and T. Wakita.** 2014. Evaluation and identification of
892 hepatitis B virus entry inhibitors using HepG2 cells overexpressing a membrane transporter
893 NTCP. Biochem Biophys Res Commun **443:**808-13.
894 18. **Kahila Bar-Gal, G., M. J. Kim, A. Klein, D. H. Shin, C. S. Oh, J. W. Kim, T. H. Kim, S. B. Kim,**
895 **P. R. Grant, O. Pappo, M. Spigelman, and D. Shouval.** 2012. Tracing hepatitis B virus to the
896 16th century in a Korean mummy. Hepatology **56:**1671-80.
897 19. **Kannan, M. B., V. Solovieva, and V. Blank.** 2012. The small MAF transcription factors MAFF,
898 MAFG and MAFK: current knowledge and perspectives. Biochim Biophys Acta **1823:**1841-6.
899 20. **Kataoka, K., K. Igarashi, K. Itoh, K. T. Fujiwara, M. Noda, M. Yamamoto, and M. Nishizawa.**
900 1995. Small Maf proteins heterodimerize with Fos and may act as competitive repressors of
901 the NF-E2 transcription factor. Mol Cell Biol **15:**2180-90.
902 21. **Kataoka, K., M. Nishizawa, and S. Kawai.** 1993. Structure-function analysis of the maf
903 oncogene product, a member of the b-Zip protein family. Journal of Virology **67:**2133-2141.
904 22. **Kataoka, K., M. Noda, and M. Nishizawa.** 1994. Maf nuclear oncoprotein recognizes
905 sequences related to an AP-1 site and forms heterodimers with both Fos and Jun. Mol Cell
906 Biol **14:**700-12.
907 23. **Katoh, K., and D. M. Standley.** 2013. MAFFT multiple sequence alignment software version
908 7: improvements in performance and usability. Mol Biol Evol **30:**772-80.
909 24. **Katsuoka, F., and M. Yamamoto.** 2016. Small Maf proteins (MafF, MafG, MafK): History,
910 structure and function. Gene **586:**197-205.
911 25. **Kerppola, T. K., and T. Curran.** 1994. A conserved region adjacent to the basic domain is
912 required for recognition of an extended DNA binding site by Maf/Nrl family proteins.
913 Oncogene **9:**3149-58.
914 26. **Kimura, M., T. Yamamoto, J. Zhang, K. Itoh, M. Kyo, T. Kamiya, H. Aburatani, F. Katsuoka,**
915 **H. Kurokawa, T. Tanaka, H. Motohashi, and M. Yamamoto.** 2007. Molecular basis

916 distinguishing the DNA binding profile of Nrf2-Maf heterodimer from that of Maf
917 homodimer. J Biol Chem **282:**33681-90.
918 27. **Krause-Kyora, B., J. Susat, F. M. Key, D. Kuhnert, E. Bosse, A. Immel, C. Rinne, S. C. Kornell,**
919 **D. Yepes, S. Franzenburg, H. O. Heyne, T. Meier, S. Losch, H. Meller, S. Friederich, N.**
920 **Nicklisch, K. W. Alt, S. Schreiber, A. Tholey, A. Herbig, A. Nebel, and J. Krause.** 2018.
921 Neolithic and medieval virus genomes reveal complex evolution of hepatitis B. Elife **7**.
922 28. **Lena Allweiss, M. Y., Barbara Testoni, Julie Lucifora, Chunkyu Ko, Bingqian Qu, Dieter**
923 **Glebe, Elena S. kim, Mark Lutgehetmann, Stephan Urban, Guofeng Cheng, William**
924 **Delaney, Massimo Levrero, Ulrike Protzer, Fabien Zoulim, Haitao Guo, Maura Dandri.** 2019.
925 Final results of the concerted harmonization efforts for HBV cccDNA quantification, 2019
926 International HBV Meeting, Melbourne, Australia.
927 29. **Liang, G., G. Liu, K. Kitamura, Z. Wang, S. Chowdhury, A. M. Monjurul, K. Wakae, M. Koura,**
928 **M. Shimadu, K. Kinoshita, and M. Muramatsu.** 2015. TGF-beta suppression of HBV RNA
929 through AID-dependent recruitment of an RNA exosome complex. PLoS Pathog
930 **11:**e1004780.
931 30. **Liu, T., L. Zhang, D. Joo, and S. C. Sun.** 2017. NF-kappaB signaling in inflammation. Signal
932 Transduct Target Ther **2**.
933 31. **Lopez-Cabrera, M., J. Letovsky, K. Q. Hu, and A. Siddiqui.** 1991. Transcriptional factor C/EBP
934 binds to and transactivates the enhancer element II of the hepatitis B virus. Virology
935 **183:**825-9.
936 32. **Massrieh, W., A. Derjuga, F. Doualla-Bell, C. Y. Ku, B. M. Sanborn, and V. Blank.** 2006.
937 Regulation of the MAFF transcription factor by proinflammatory cytokines in myometrial
938 cells. Biol Reprod **74:**699-705.
939 33. **Meurs, E. F., Y. Watanabe, S. Kadereit, G. N. Barber, M. G. Katze, K. Chong, B. R. Williams,**
940 **and A. G. Hovanessian.** 1992. Constitutive expression of human double-stranded RNA-
941 activated p68 kinase in murine cells mediates phosphorylation of eukaryotic initiation factor
942 2 and partial resistance to encephalomyocarditis virus growth. J Virol **66:**5805-14.
943 34. **Meyerson, N. R., L. Zhou, Y. R. Guo, C. Zhao, Y. J. Tao, R. M. Krug, and S. L. Sawyer.** 2017.
944 Nuclear TRIM25 Specifically Targets Influenza Virus Ribonucleoproteins to Block the Onset
945 of RNA Chain Elongation. Cell Host Microbe **22:**627-638 e7.
946 35. **Migita, K., Y. Maeda, S. Abiru, M. Nakamura, A. Komori, S. Miyazoe, K. Nakao, H.**
947 **Yatsuhashi, K. Eguchi, and H. Ishibashi.** 2007. Polymorphisms of interleukin-1beta in
948 Japanese patients with hepatitis B virus infection. J Hepatol **46:**381-6.
949 36. **Mitra, B., J. Wang, E. S. Kim, R. Mao, M. Dong, Y. Liu, J. Zhang, and H. Guo.** 2019. Hepatitis
950 B Virus Precore Protein p22 Inhibits Alpha Interferon Signaling by Blocking STAT Nuclear
951 Translocation. J Virol **93**.
952 37. **Mogilenko, D. A., E. B. Dizhe, V. S. Shavva, I. A. Lapikov, S. V. Orlov, and A. P.**
953 **Perevozchikov.** 2009. Role of the nuclear receptors HNF4 alpha, PPAR alpha, and LXRs in
954 the TNF alpha-mediated inhibition of human apolipoprotein A-I gene expression in HepG2
955 cells. Biochemistry **48:**11950-60.
956 38. **Moolla, N., M. Kew, and P. Arbuthnot.** 2002. Regulatory elements of hepatitis B virus
957 transcription. J Viral Hepat **9:**323-31.
958 39. **Motohashi, H., F. Katsuoka, J. A. Shavit, J. D. Engel, and M. Yamamoto.** 2000. Positive or
959 negative MARE-dependent transcriptional regulation is determined by the abundance of
960 small Maf proteins. Cell **103:**865-75.

961 40. **Motohashi, H., T. O'Connor, F. Katsuoka, J. D. Engel, and M. Yamamoto.** 2002. Integration
962 and diversity of the regulatory network composed of Maf and CNC families of transcription
963 factors. Gene **294:**1-12.
964 41. **Motohashi, H., J. A. Shavit, K. Igarashi, M. Yamamoto, and J. D. Engel.** 1997. The world
965 according to Maf. Nucleic Acids Res **25:**2953-59.
966 42. **Muhlemann, B., T. C. Jones, P. B. Damgaard, M. E. Allentoft, I. Shevnina, A. Logvin, E.**
967 **Usmanova, I. P. Panyushkina, B. Boldgiv, T. Bazartseren, K. Tashbaeva, V. Merz, N. Lau, V.**
968 **Smrcka, D. Voyakin, E. Kitov, A. Epimakhov, D. Pokutta, M. Vicze, T. D. Price, V. Moiseyev,**
969 **A. J. Hansen, L. Orlando, S. Rasmussen, M. Sikora, L. Vinner, A. Osterhaus, D. J. Smith, D.**
970 **Glebe, R. A. M. Fouchier, C. Drosten, K. G. Sjogren, K. Kristiansen, and E. Willerslev.** 2018.
971 Ancient hepatitis B viruses from the Bronze Age to the Medieval period. Nature **557:**418-
972 423.
973 43. **Nassal, M.** 2015. HBV cccDNA: viral persistence reservoir and key obstacle for a cure of
974 chronic hepatitis B. Gut **64:**1972-84.
975 44. **Ney, P. A., B. P. Sorrentino, C. H. Lowrey, and A. W. Nienhuis.** 1990. Inducibility of the HS
976 II enhancer depends on binding of an erythroid specific nuclear protein. Nucleic Acids Res
977 **18:**6011-7.
978 45. **Nishitsuji, H., S. Ujino, Y. Shimizu, K. Harada, J. Zhang, M. Sugiyama, M. Mizokami, and K.**
979 **Shimotohno.** 2015. Novel reporter system to monitor early stages of the hepatitis B virus
980 life cycle. Cancer Sci **106:**1616-24.
981 46. **Orzalli, M. H., and D. M. Knipe.** 2014. Cellular sensing of viral DNA and viral evasion
982 mechanisms. Annu Rev Microbiol **68:**477-92.
983 47. **Paraskevis, D., G. Magiorkinis, E. Magiorkinis, S. Y. Ho, R. Belshaw, J. P. Allain, and A.**
984 **Hatzakis.** 2013. Dating the origin and dispersal of hepatitis B virus infection in humans and
985 primates. Hepatology **57:**908-16.
986 48. **Park, Y. K., E. S. Park, D. H. Kim, S. H. Ahn, S. H. Park, A. R. Lee, S. Park, H. S. Kang, J. H. Lee,**
987 **J. M. Kim, S. K. Lee, K. H. Lim, N. Isorce, S. Tong, F. Zoulim, and K. H. Kim.** 2016. Cleaved c-
988 FLIP mediates the antiviral effect of TNF-alpha against hepatitis B virus by dysregulating
989 hepatocyte nuclear factors. J Hepatol **64:**268-277.
990 49. **Patterson Ross, Z., J. Klunk, G. Fornaciari, V. Giuffra, S. Duchene, A. T. Duggan, D. Poinar,**
991 **M. W. Douglas, J. S. Eden, E. C. Holmes, and H. N. Poinar.** 2018. The paradox of HBV
992 evolution as revealed from a 16th century mummy. PLoS Pathog **14:**e1006750.
993 50. **Qu, B., Y. Ni, F. A. Lempp, F. W. R. Vondran, and S. Urban.** 2018. T5 Exonuclease Hydrolysis
994 of Hepatitis B Virus Replicative Intermediates Allows Reliable Quantification and Fast Drug
995 Efficacy Testing of Covalently Closed Circular DNA by PCR. J Virol **92**.
996 51. **Quarleri, J.** 2014. Core promoter: a critical region where the hepatitis B virus makes
997 decisions. World J Gastroenterol **20:**425-35.
998 52. **Raney, A. K., J. L. Johnson, C. N. Palmer, and A. McLachlan.** 1997. Members of the nuclear
999 receptor superfamily regulate transcription from the hepatitis B virus nucleocapsid
1000 promoter. J Virol **71:**1058-71.
1001 53. **Rushmore, T. H., M. R. Morton, and C. B. Pickett.** 1991. The antioxidant responsive element.
1002 Activation by oxidative stress and identification of the DNA consensus sequence required
1003 for functional activity. J Biol Chem **266:**11632-9.
1004 54. **Sakurai, F., S. Mitani, T. Yamamoto, K. Takayama, M. Tachibana, K. Watashi, T. Wakita, S.**
1005 **Iijima, Y. Tanaka, and H. Mizuguchi.** 2017. Human induced-pluripotent stem cell-derived

1006 hepatocyte-like cells as an in vitro model of human hepatitis B virus infection. Sci Rep
1007 **7:**45698.
1008 55. **Sandelin, A., W. Alkema, P. Engstrom, W. W. Wasserman, and B. Lenhard.** 2004. JASPAR:
1009 an open-access database for eukaryotic transcription factor binding profiles. Nucleic Acids
1010 Res **32:**D91-4.
1011 56. **Schoggins, J. W., D. A. MacDuff, N. Imanaka, M. D. Gainey, B. Shrestha, J. L. Eitson, K. B.**
1012 **Mar, R. B. Richardson, A. V. Ratushny, V. Litvak, R. Dabelic, B. Manicassamy, J. D. Aitchison,**
1013 **A. Aderem, R. M. Elliott, A. Garcia-Sastre, V. Racaniello, E. J. Snijder, W. M. Yokoyama, M.**
1014 **S. Diamond, H. W. Virgin, and C. M. Rice.** 2014. Pan-viral specificity of IFN-induced genes
1015 reveals new roles for cGAS in innate immunity. Nature **505:**691-5.
1016 57. **Schreiner, S., S. Kinkley, C. Burck, A. Mund, P. Wimmer, T. Schubert, P. Groitl, H. Will, and**
1017 **T. Dobner.** 2013. SPOC1-mediated antiviral host cell response is antagonized early in human
1018 adenovirus type 5 infection. PLoS Pathog **9:**e1003775.
1019 58. **Shiromoto, F., H. H. Aly, H. Kudo, K. Watashi, A. Murayama, N. Watanabe, X. Zheng, T.**
1020 **Kato, K. Chayama, M. Muramatsu, and T. Wakita.** 2018. IL-1beta/ATF3-mediated induction
1021 of Ski2 expression enhances hepatitis B virus x mRNA degradation. Biochem Biophys Res
1022 Commun **503:**1854-1860.
1023 59. **Sugiyama, M., Y. Tanaka, T. Kato, E. Orito, K. Ito, S. K. Acharya, R. G. Gish, A. Kramvis, T.**
1024 **Shimada, N. Izumi, M. Kaito, Y. Miyakawa, and M. Mizokami.** 2006. Influence of hepatitis
1025 B virus genotypes on the intra- and extracellular expression of viral DNA and antigens.
1026 Hepatology **44:**915-24.
1027 60. **Sun, J., A. Muto, H. Hoshino, A. Kobayashi, S. Nishimura, M. Yamamoto, N. Hayashi, E. Ito,**
1028 **and K. Igarashi.** 2001. The promoter of mouse transcription repressor bach1 is regulated by
1029 Sp1 and trans-activated by Bach1. J Biochem **130:**385-92.
1030 61. **Thomas, H., S. Senkel, S. Erdmann, T. Arndt, G. Turan, L. Klein-Hitpass, and G. U. Ryffel.**
1031 2004. Pattern of genes influenced by conditional expression of the transcription factors
1032 HNF6, HNF4alpha and HNF1beta in a pancreatic beta-cell line. Nucleic Acids Res **32:**e150.
1033 62. **Wang, H., S. Kim, and W. S. Ryu.** 2009. DDX3 DEAD-Box RNA helicase inhibits hepatitis B
1034 virus reverse transcription by incorporation into nucleocapsids. J Virol **83:**5815-24.
1035 63. **Wang, H., P. Maechler, P. A. Antinozzi, K. A. Hagenfeldt, and C. B. Wollheim.** 2000.
1036 Hepatocyte nuclear factor 4alpha regulates the expression of pancreatic beta -cell genes
1037 implicated in glucose metabolism and nutrient-induced insulin secretion. J Biol Chem
1038 **275:**35953-9.
1039 64. **Wang, Y., L. Cui, G. Yang, J. Zhan, L. Guo, Y. Chen, C. Fan, D. Liu, and D. Guo.** 2019. Hepatitis
1040 B e Antigen Inhibits NF-kappaB Activity by Interrupting K63-Linked Ubiquitination of NEMO.
1041 J Virol **93**.
1042 65. **Watashi, K., G. Liang, M. Iwamoto, H. Marusawa, N. Uchida, T. Daito, K. Kitamura, M.**
1043 **Muramatsu, H. Ohashi, T. Kiyohara, R. Suzuki, J. Li, S. Tong, Y. Tanaka, K. Murata, H. Aizaki,**
1044 **and T. Wakita.** 2013. Interleukin-1 and tumor necrosis factor-alpha trigger restriction of
1045 hepatitis B virus infection via a cytidine deaminase activation-induced cytidine deaminase
1046 (AID). J Biol Chem **288:**31715-27.
1047 66. **Wieland, S., R. Thimme, R. H. Purcell, and F. V. Chisari.** 2004. Genomic analysis of the host
1048 response to hepatitis B virus infection. Proc Natl Acad Sci U S A **101:**6669-74.

1049 67. **Wustenhagen, E., F. Boukhallouk, I. Negwer, K. Rajalingam, F. Stubenrauch, and L. Florin.**
1050 2018. The Myb-related protein MYPOP is a novel intrinsic host restriction factor of
1051 oncogenic human papillomaviruses. Oncogene **37:**6275-6284.
1052 68. **Xia, Y., D. Stadler, J. Lucifora, F. Reisinger, D. Webb, M. Hosel, T. Michler, K. Wisskirchen,**
1053 **X. Cheng, K. Zhang, W. M. Chou, J. M. Wettengel, A. Malo, F. Bohne, D. Hoffmann, F. Eyer,**
1054 **R. Thimme, C. S. Falk, W. E. Thasler, M. Heikenwalder, and U. Protzer.** 2016. Interferon-
1055 gamma and Tumor Necrosis Factor-alpha Produced by T Cells Reduce the HBV Persistence
1056 Form, cccDNA, Without Cytolysis. Gastroenterology **150:**194-205.
1057 69. **Yu, X., and J. E. Mertz.** 1997. Differential regulation of the pre-C and pregenomic promoters
1058 of human hepatitis B virus by members of the nuclear receptor superfamily. J Virol **71:**9366-
1059 74.
1060 70. **Yu, Y., P. Wan, Y. Cao, W. Zhang, J. Chen, L. Tan, Y. Wang, Z. Sun, Q. Zhang, Y. Wan, Y. Zhu,**
1061 **F. Liu, K. Wu, Y. Liu, and J. Wu.** 2017. Hepatitis B Virus e Antigen Activates the Suppressor
1062 of Cytokine Signaling 2 to Repress Interferon Action. Sci Rep **7:**1729.
1063 71. **Zhou, W., Y. Ma, J. Zhang, J. Hu, M. Zhang, Y. Wang, Y. Li, L. Wu, Y. Pan, Y. Zhang, X. Zhang,**
1064 **Z. Zhang, H. Li, L. Lu, L. Jin, J. Wang, Z. Yuan, and J. Liu.** 2017. Predictive model for
1065 inflammation grades of chronic hepatitis B: Large-scale analysis of clinical parameters and
1066 gene expressions. Liver Int **37:**1632-1641.

1067

1068

Fig. 1

A

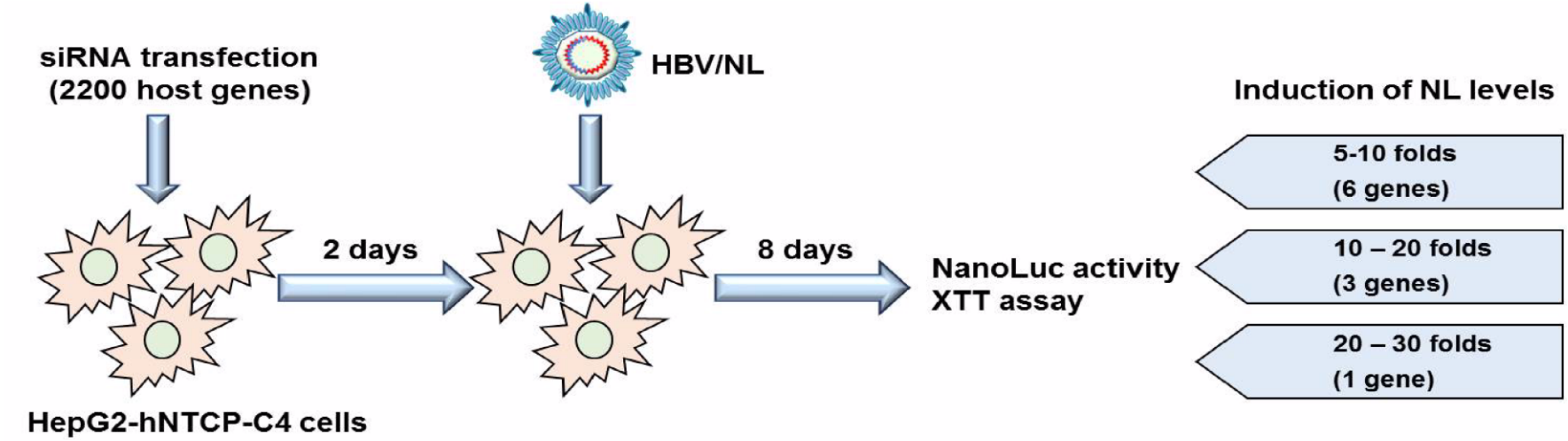
siRNA transfection
(2200 host genes)
HBV/NL
Induction of NL levels
5-10 folds
(6 genes)
2 days
8 days
NanoLuc activity
XTT assay
10 – 20 folds
(3 genes)
20 – 30 folds
(1 gene)
HepG2-hNTCP-C4 cells

B

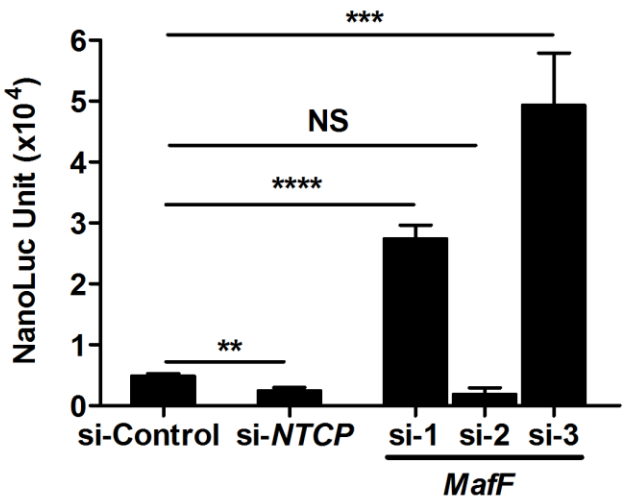
***
NS
****
**
NanoLuc Unit (x10^4)
0
1
2
3
4
5
6
si-Control
si-NTCP
si-1
si-2
si-3
MafF

C

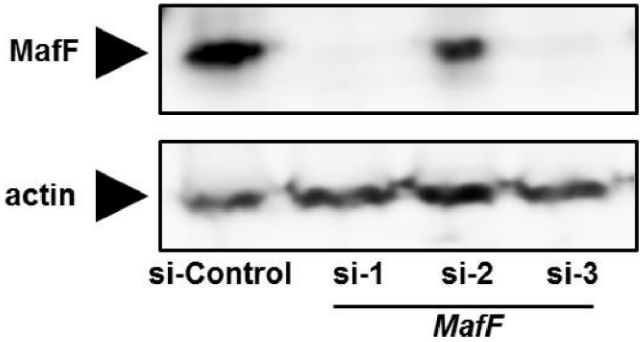
MafF
actin
si-Control
si-1
si-2
si-3
MafF

D

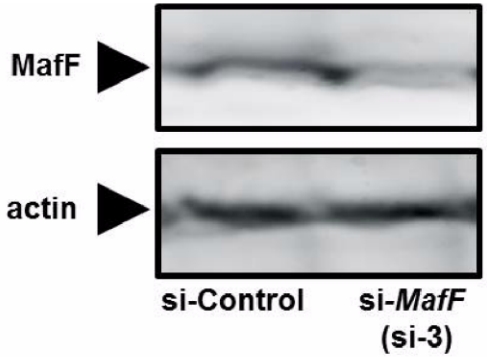
MafF
actin
si-Control
si-MafF
(si-3)

Fig. 2

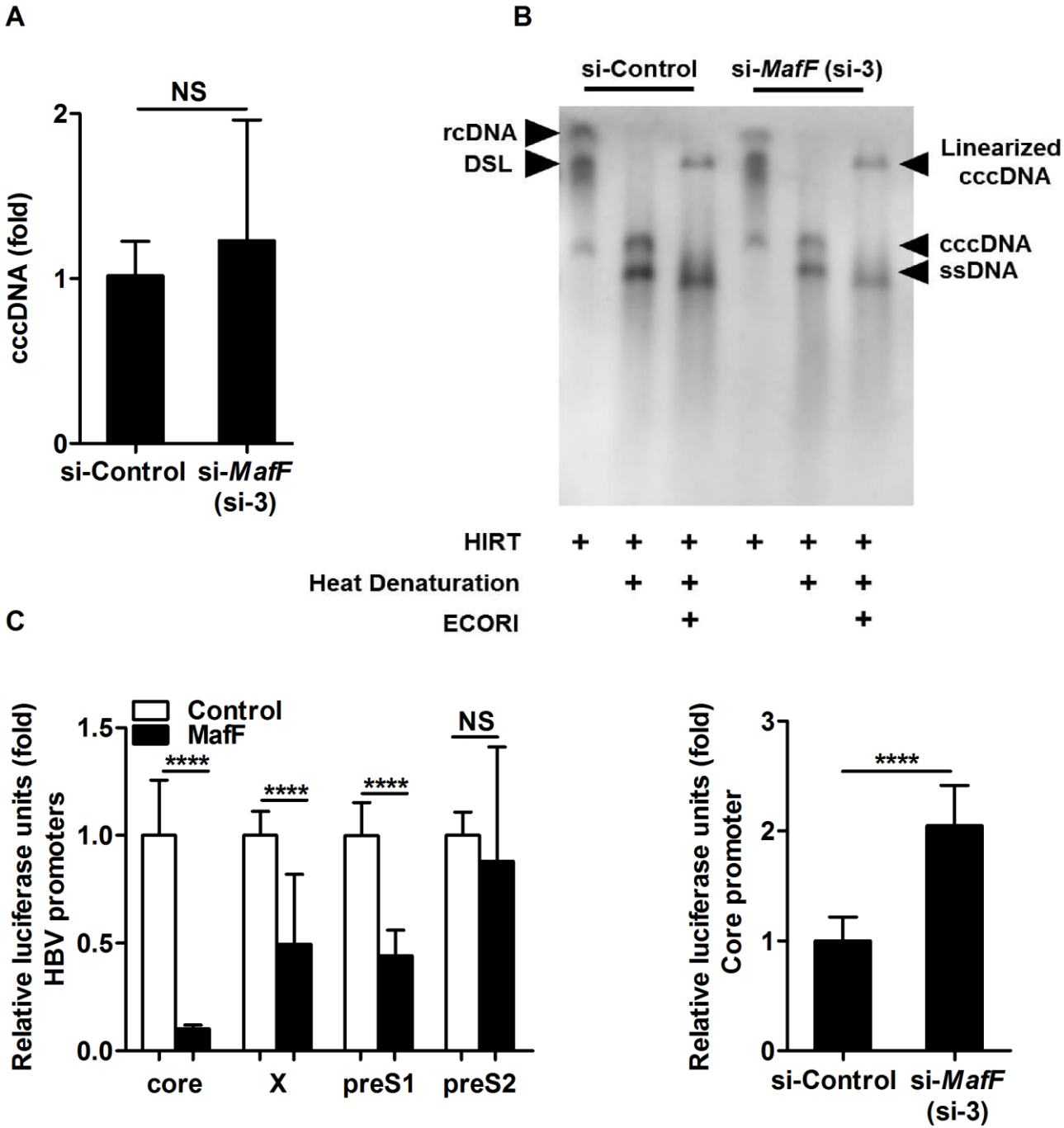
A
NS
cccDNA (fold)
2
1
0
si-Control
si-MafF (si-3)
B
si-Control
si-MafF (si-3)
rcDNA
DSL
Linearized cccDNA
cccDNA
ssDNA
HIRT
Heat Denaturation
ECORI
C
Control
MafF
Relative luciferase units (fold) HBV promoters
1.5
1.0
0.5
0.0
****
****
****
NS
core
X
preS1
preS2
Relative luciferase units (fold) Core promoter
3
2
1
0
****
si-Control
si-MafF (si-3)

Fig. 3

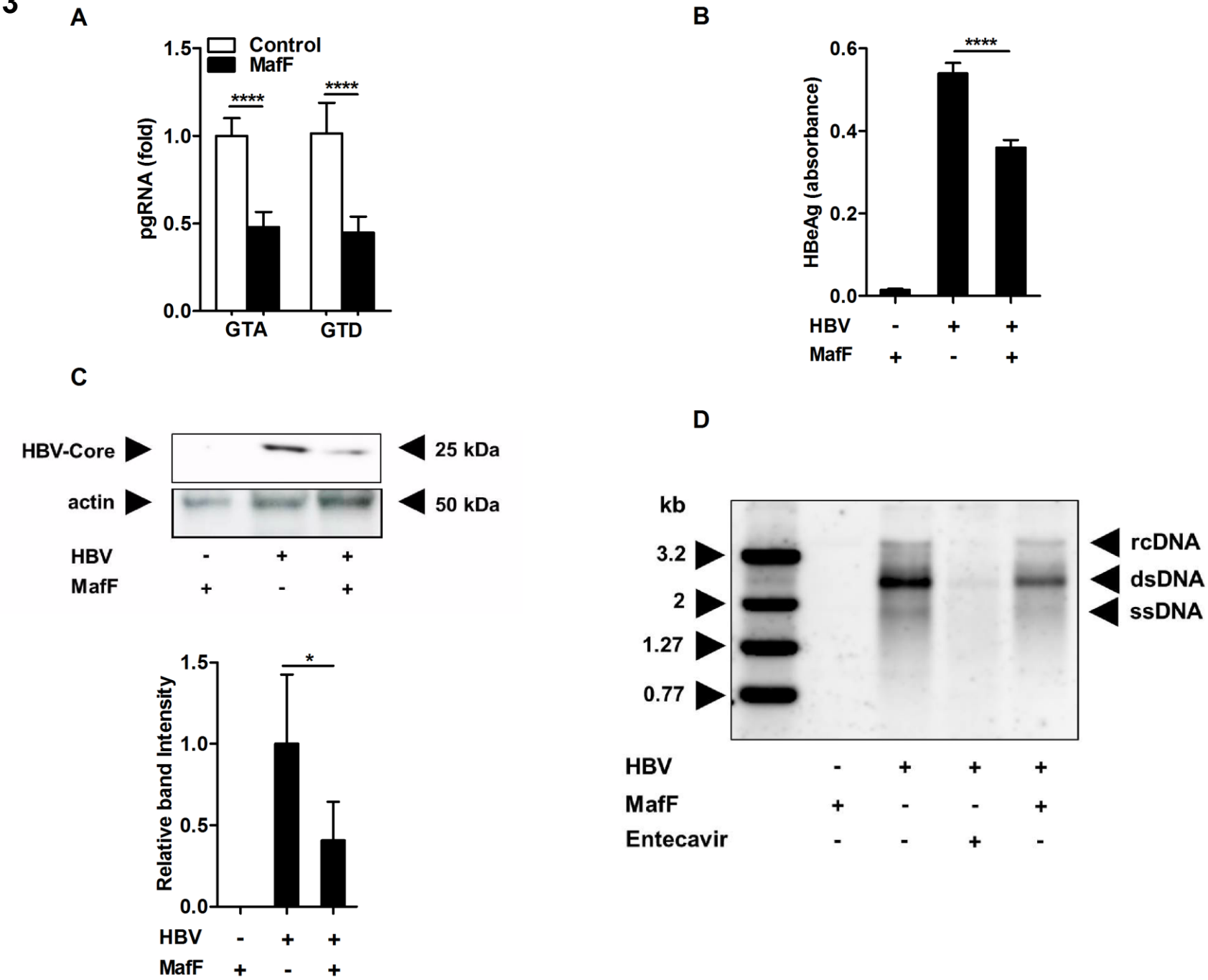
A
Control
MafF
pgRNA (fold)
1.5
1.0
0.5
0.0
****
****
GTA
GTD
B
HBeAg (absorbance)
0.6
0.4
0.2
0.0
****
HBV - + +
MafF + - +
C
HBV-Core
actin
25 kDa
50 kDa
HBV - + +
MafF + - +
Relative band Intensity
1.5
1.0
0.5
0.0
*
HBV - + +
MafF + - +
D
kb
3.2
2
1.27
0.77
rcDNA
dsDNA
ssDNA
HBV - + + +
MafF + - - +
Entecavir - - + -

Fig. 4

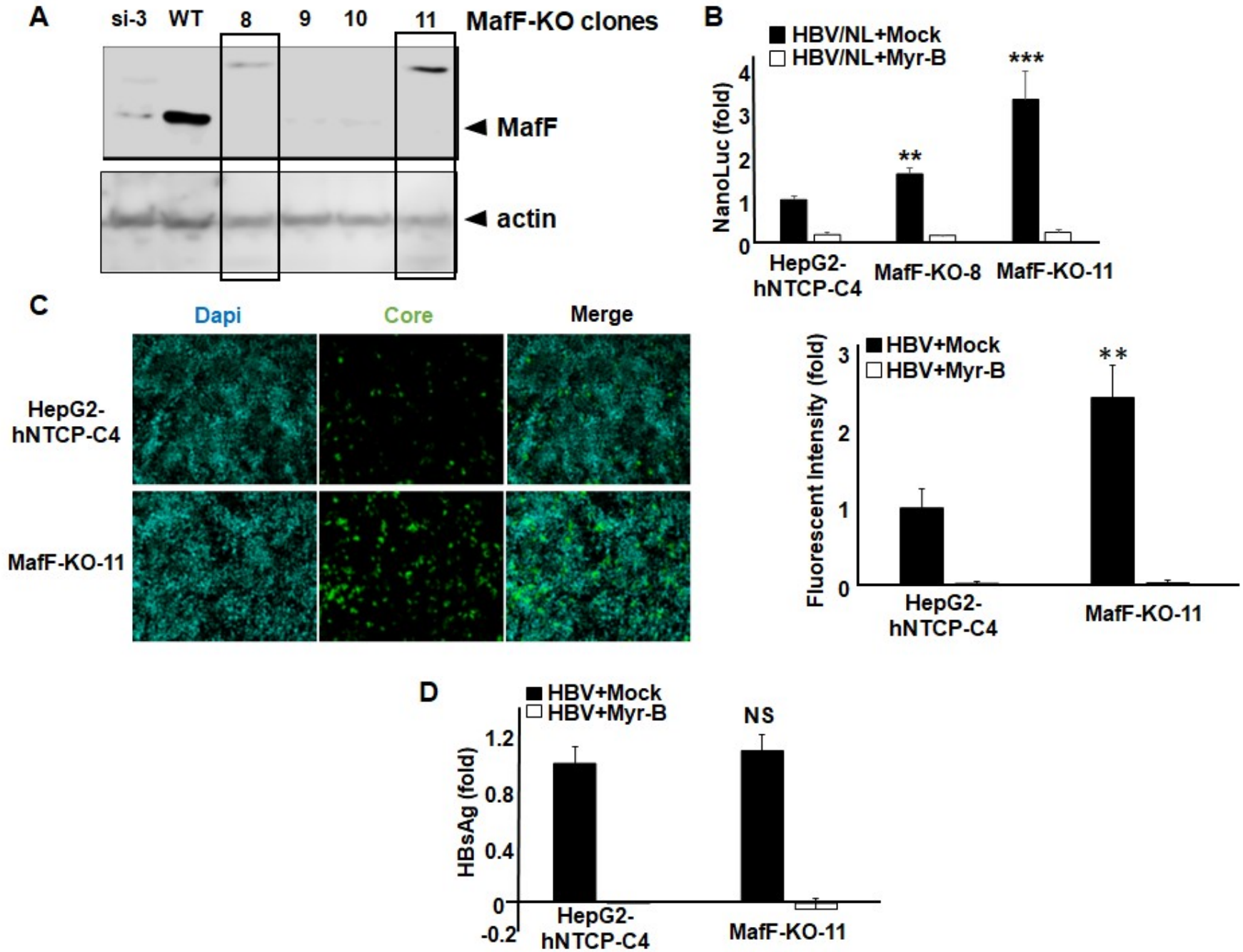
A
si-3
WT
8
9
10
11
MafF-KO clones
MafF
actin
B
HBV/NL+Mock
HBV/NL+Myr-B
NanoLuc (fold)
0
1
2
3
4
**
***
HepG2-hNTCP-C4
MafF-KO-8
MafF-KO-11
C
Dapi
Core
Merge
HepG2-hNTCP-C4
MafF-KO-11
HBV+Mock
HBV+Myr-B
Fluorescent Intensity (fold)
0
1
2
3
**
HepG2-hNTCP-C4
MafF-KO-11
D
HBV+Mock
HBV+Myr-B
HBsAg (fold)
-0.2
0
0.4
0.8
1.2
NS
HepG2-hNTCP-C4
MafF-KO-11

Fig. 5

A

TGGACTCTCAGCA	HBV-GTC (nt1667-1679)
* * * * * * ** * *C * A *	HBV-GTC (mutation generated in this study)
TGCT * * * - - * * * * * *	MARE
GT * * * - - * * * * * *	Bach1
AT * * * - - * * * * * *	Bach2
AT * * * - - * * * * * *	Nrf2
GC *C * - - *GC * * *	Nrf1

B

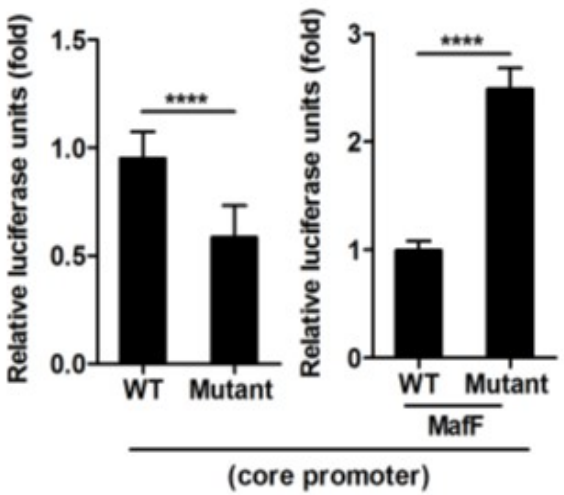

C

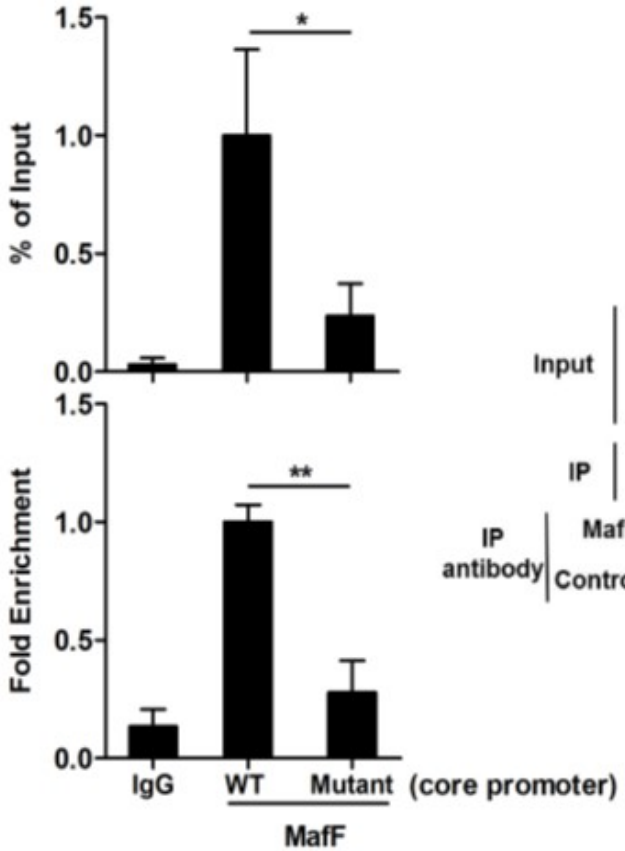

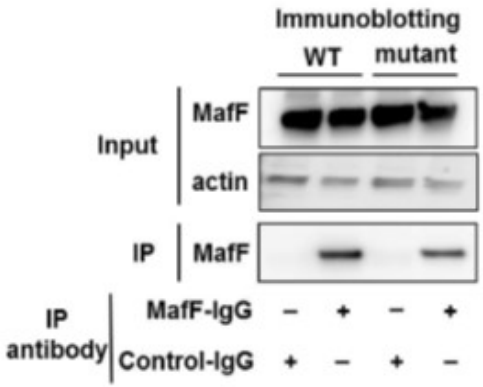

D

Seqlogo at MARE region

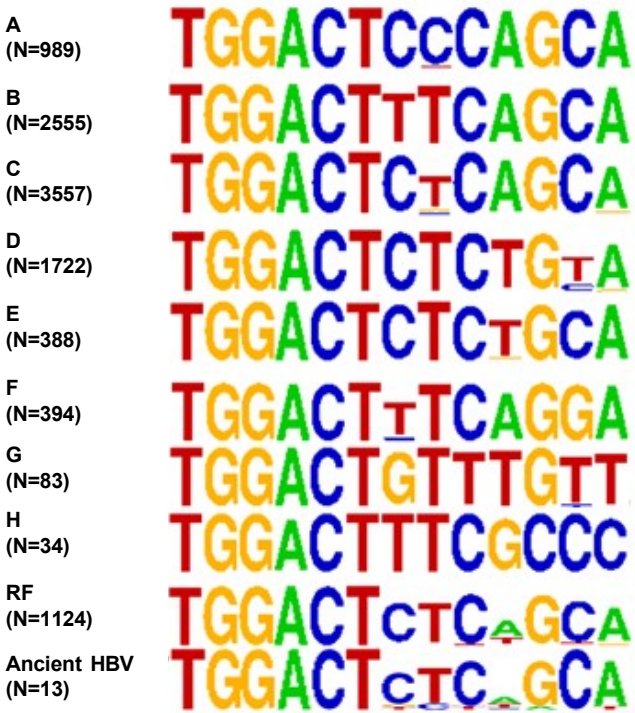

Fig. 6

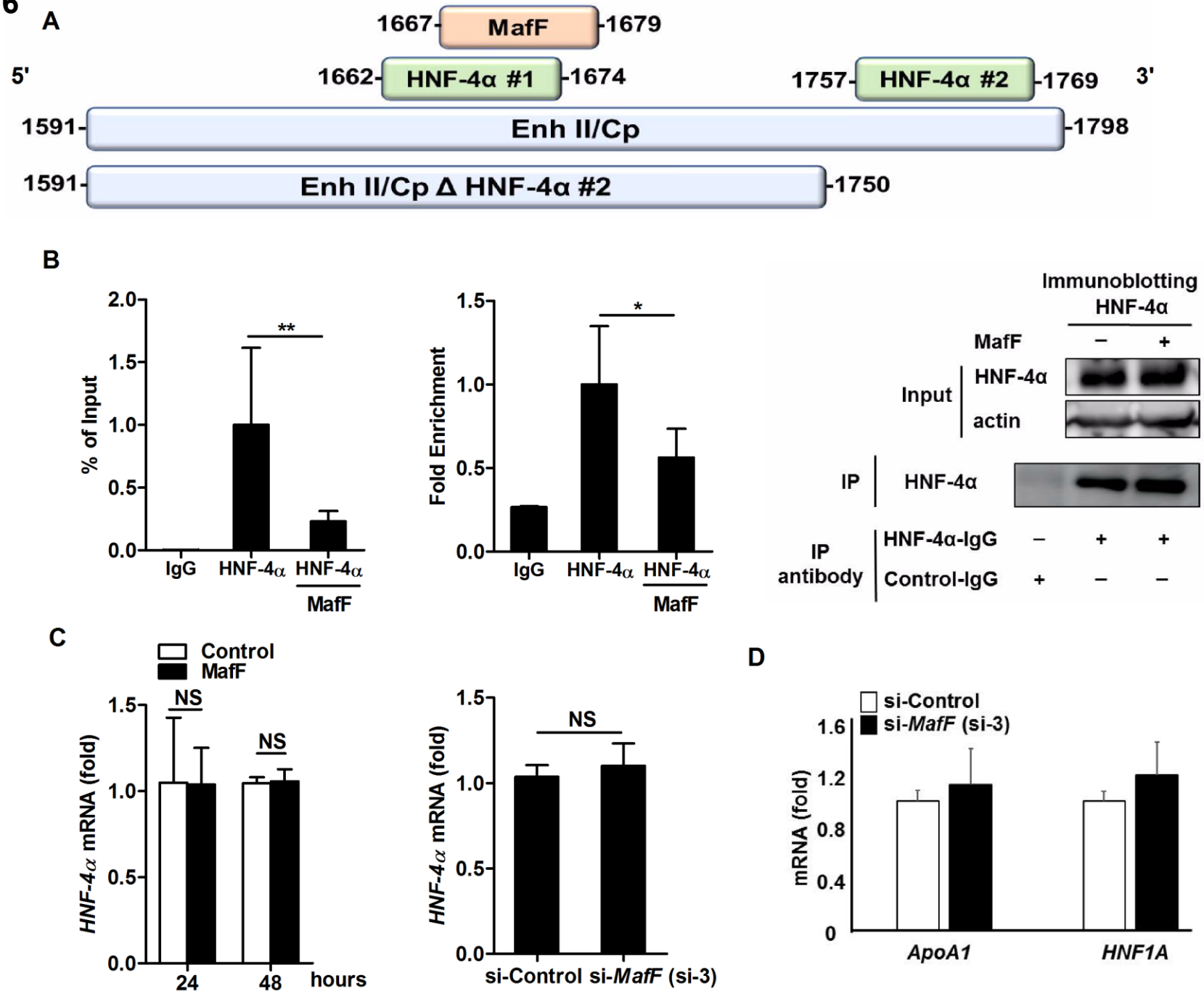
A
1667-
MafF
-1679
5'
1662-
HNF-4α #1
-1674
1757-
HNF-4α #2
-1769
3'
1591-
Enh II/Cp
-1798
1591-
Enh II/Cp Δ HNF-4α #2
-1750
B
% of Input
2.0
1.5
1.0
0.5
0.0
**
IgG
HNF-4α
HNF-4α
MafF
Fold Enrichment
1.5
1.0
0.5
0.0
*
IgG
HNF-4α
HNF-4α
MafF
Immunoblotting
HNF-4α
MafF
–
+
Input
HNF-4α
actin
IP
HNF-4α
IP antibody
HNF-4α-IgG
–
+
+
Control-IgG
+
–
–
C
Control
MafF
HNF-4α mRNA (fold)
1.5
1.0
0.5
0.0
NS
NS
24
48
hours
HNF-4α mRNA (fold)
1.5
1.0
0.5
0.0
NS
si-Control
si-MafF (si-3)
D
si-Control
si-MafF (si-3)
mRNA (fold)
1.6
1.2
0.8
0.4
0
ApoA1
HNF1A

Fig. 7

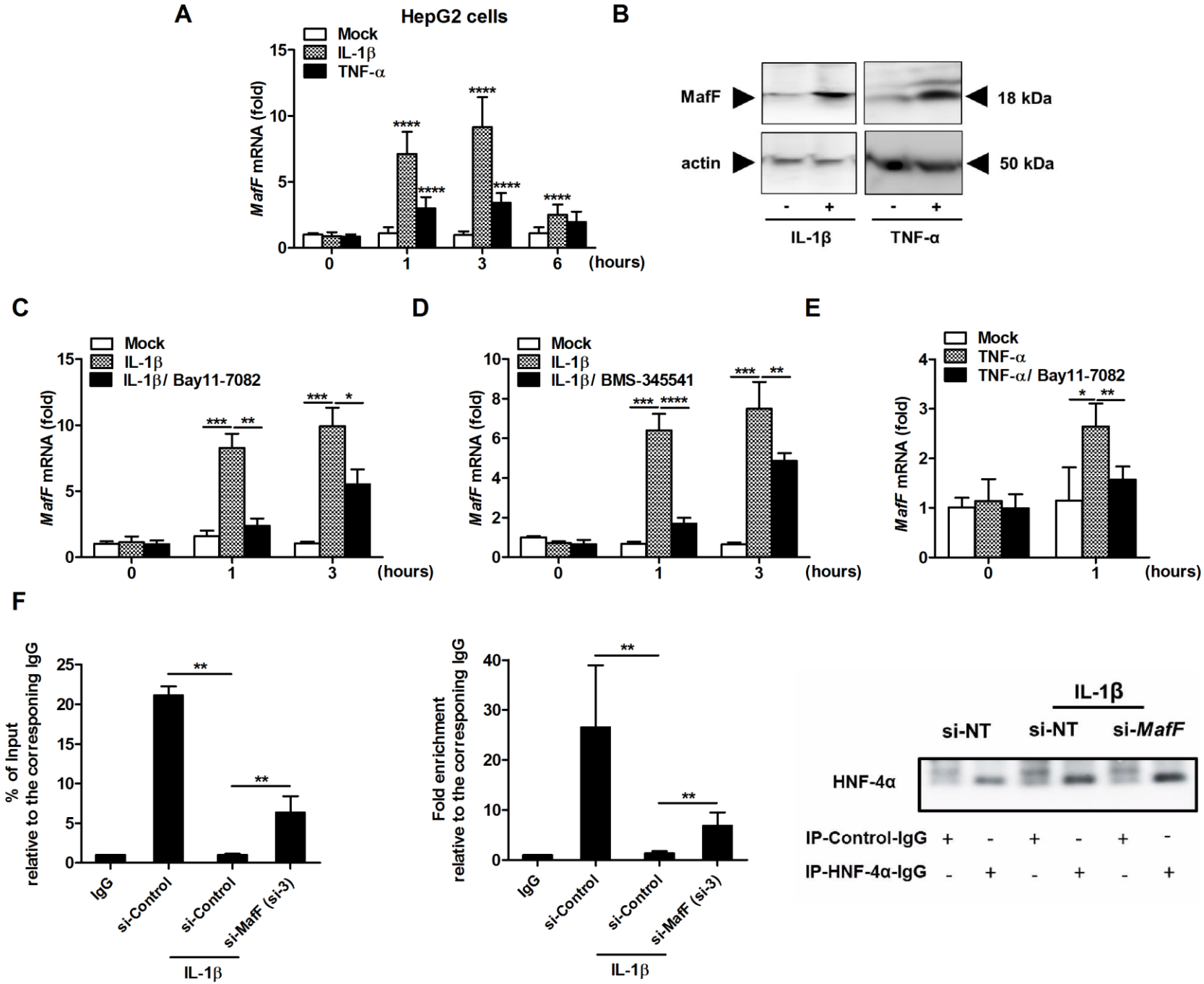
A
HepG2 cells
Mock
IL-1β
TNF-α
MafF mRNA (fold)
(hours)
B
MafF
actin
18 kDa
50 kDa
IL-1β
TNF-α
C
IL-1β/ Bay11-7082
D
IL-1β/ BMS-345541
E
TNF-α/ Bay11-7082
F
% of Input relative to the corresponing IgG
Fold enrichment relative to the corresponing IgG
IgG
si-Control
si-MafF (si-3)
si-NT
si-MafF
HNF-4α
IP-Control-IgG
IP-HNF-4α-IgG

Fig. 8

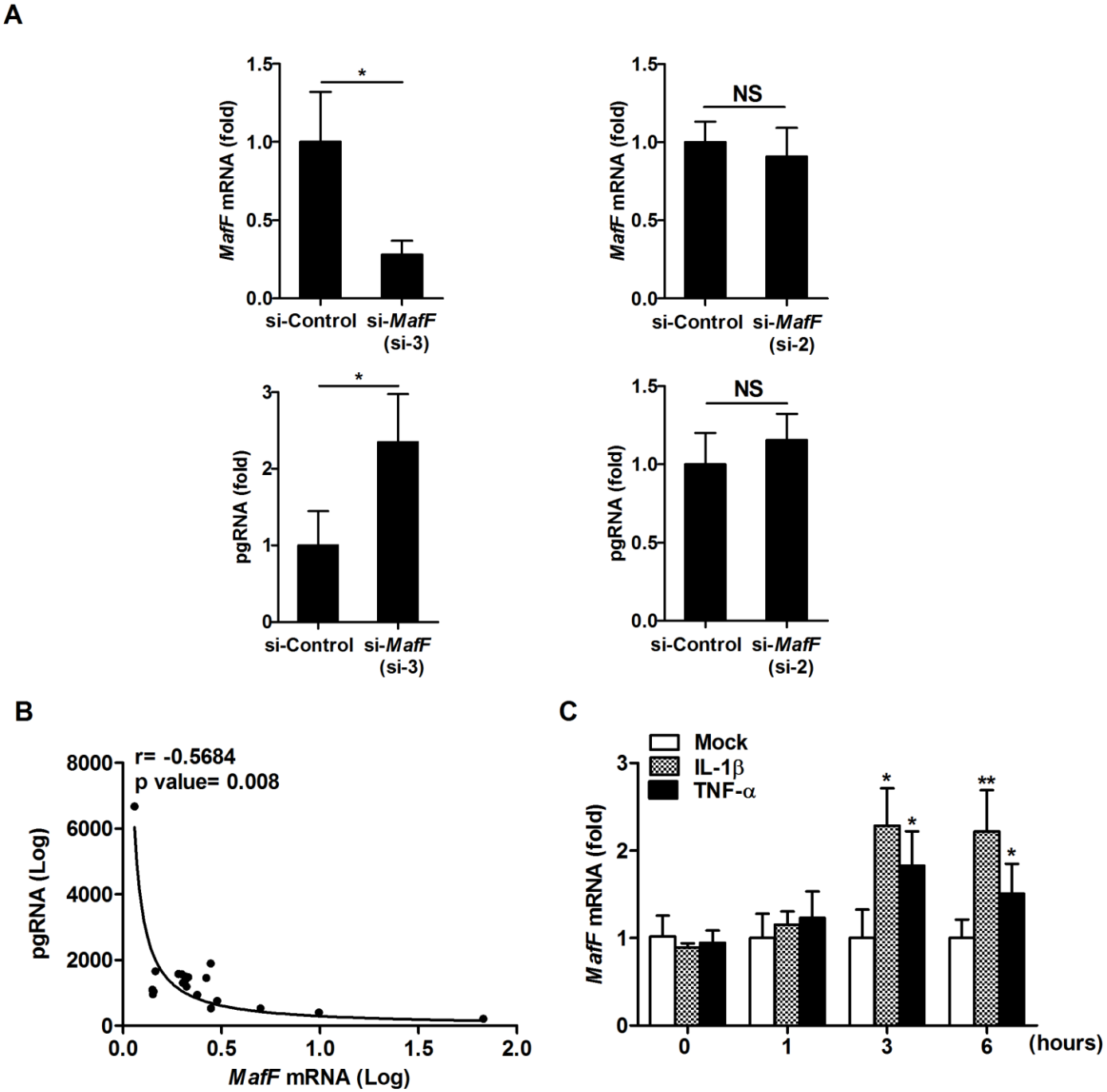
A
MafF mRNA (fold)
1.5
1.0
0.5
0.0
*
si-Control
si-MafF (si-3)
NS
si-MafF (si-2)
pgRNA (fold)
3
2
1
0
B
r= -0.5684
p value= 0.008
8000
6000
4000
2000
0
pgRNA (Log)
0.0
0.5
1.0
1.5
2.0
MafF mRNA (Log)
C
Mock
IL-1β
TNF-α
**
0
1
3
6
(hours)

Fig. 9

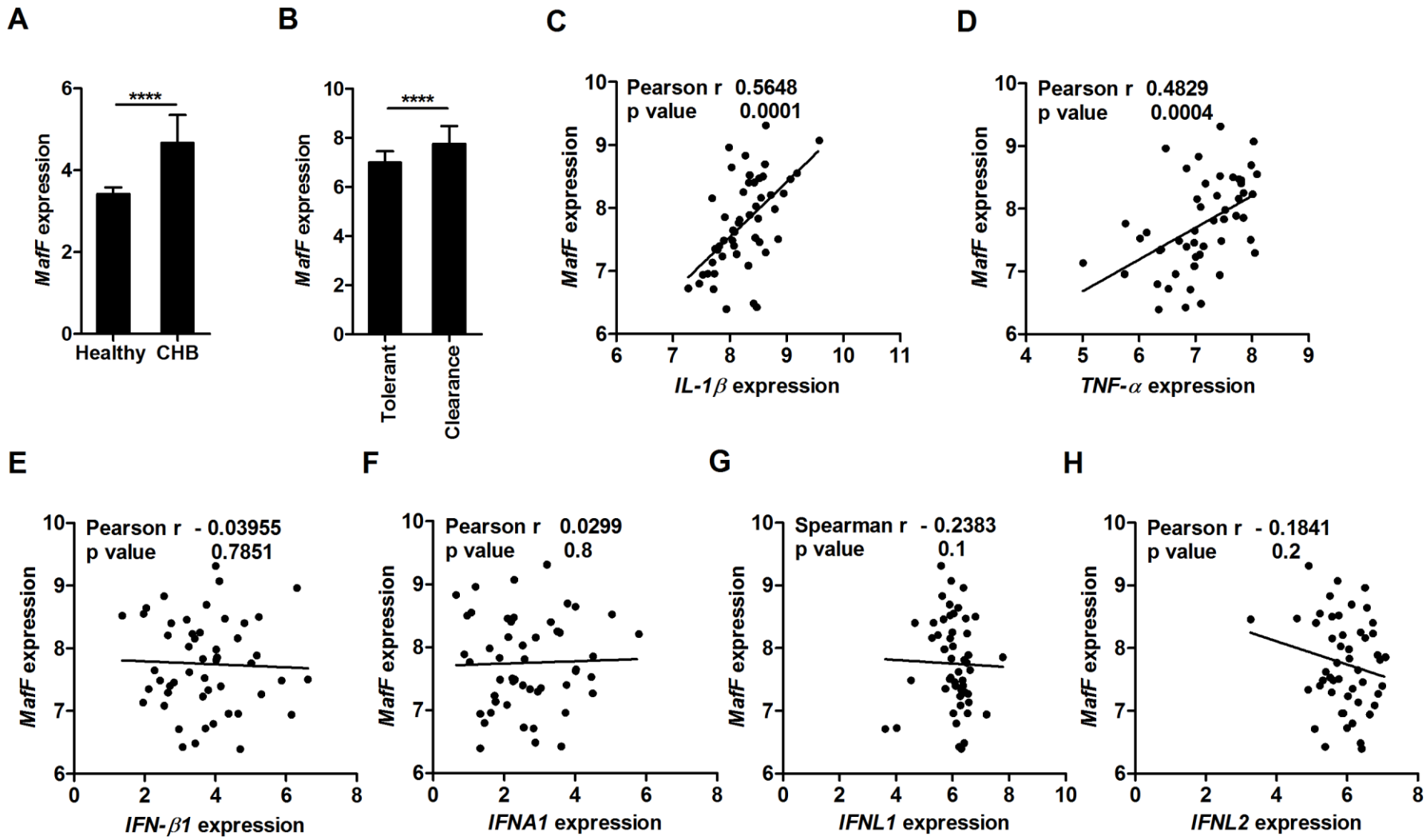
A
MafF expression
****
Healthy
CHB
B
MafF expression
****
Tolerant
Clearance
C
Pearson r 0.5648
p value 0.0001
MafF expression
IL-1β expression
D
Pearson r 0.4829
p value 0.0004
MafF expression
TNF-α expression
E
Pearson r - 0.03955
p value 0.7851
MafF expression
IFN-β1 expression
F
Pearson r 0.0299
p value 0.8
MafF expression
IFNA1 expression
G
Spearman r - 0.2383
p value 0.1
MafF expression
IFNL1 expression
H
Pearson r - 0.1841
p value 0.2
MafF expression
IFNL2 expression